Cerebral Cortex, May 2019;29: 2125–2139

doi: 10.1093/cercor/bhy094
Advance Access Publication Date: 24 April 2018
Original Article

ORIGINAL ARTICLE

Ethanol Exposure *In Utero* Disrupts Radial Migration and Pyramidal Cell Development in the Somatosensory Cortex

Laurie C. Delatour, Pamela W. Yeh and Hermes H. Yeh

Program in Experimental and Molecular Medicine, Department of Molecular and Systems Biology, Geisel School of Medicine at Dartmouth, 66 College Street, Hanover, NH 03755, USA

Address correspondence to Hermes H. Yeh, Department of Molecular and Systems Biology, Geisel School of Medicine at Dartmouth, 66 College Street, Hanover, NH 03755, USA. Email: hermes.yeh@dartmouth.edu

Abstract

Deficits in sensory processing in Fetal Alcohol Spectrum Disorders (FASD) implicate dysfunction in the somatosensory cortex. However, the effects of prenatal ethanol exposure on the development of this region await elucidation. Here, we used an established mouse model of FASD with binge-type ethanol exposure from embryonic day 13.5–16.5 to investigate the effects of prenatal ethanol exposure on pyramidal neurons in the somatosensory cortex. Specifically, we focused on the radial migration of primordial pyramidal neurons during embryonic corticogenesis and their morphology and function during active synaptogenesis in early postnatal development. We found that prenatal ethanol exposure resulted in aberrant radial migration, particularly affecting the populations of postmitotic pyramidal neurons. In addition, there was an enduring effect of prenatal ethanol exposure on glutamate-mediated synaptic transmission in layer V/VI pyramidal neurons. This persisted beyond a transient decrease in pyramidal neuron dendritic complexity that was evident only during early postnatal development. Adolescent mice exposed prenatally to ethanol also displayed decreased tactile sensitivity, as revealed by a modified adhesive tape removal assay. Our findings demonstrate the persistent effects of binge-type *in utero* ethanol exposure on pyramidal neuron form and function and ultimately sensory processing, the latter being reminiscent of that seen in individuals with FASD.

Key words: corticogenesis, FASD, gestational binge-ethanol, pyramidal neuron morphology, synaptic transmission

Introduction

In utero exposure to alcohol (ethanol) can lead to Fetal Alcohol Spectrum Disorders (FASD), an umbrella term defined based on a cadre of physical and behavioral abnormalities of varying severities (Astley and Clarren 2000; Astley 2013). In the USA, 1 in 10 pregnant women reports ethanol consumption, and 1 in 33 reports binge drinking episodes in the past 30 days (Tan et al. 2015). A binge-pattern of drinking is particularly risky since the fetus is exposed to abrupt surges of high blood alcohol levels (Maier and West 2001). In the present study, we employed an established mouse model of *in utero* binge-type ethanol exposure (Skorput et al. 2015) to investigate the effects of prenatal ethanol exposure on cortical development and function.

Diagnostic measures and management of the cognitive and behavioral deficits associated with FASD are feasible only after birth. However, the ethanol-induced aberrances underlying FASD occur ostensibly during the embryonic period, when the developing brain is highly susceptible to insult (Andersen 2003). In this light, both *in utero* chronic and binge-type ethanol exposure disrupt the corticopetal tangential migration of primordial GABAergic cortical interneurons from the medial ganglionic eminence in the subpallium to the embryonic cortex (Cuzon et al. 2008; Skorput et al. 2015). The aberrant tangential

migration is associated with an inhibitory/excitatory synaptic imbalance and deficits in executive function as well as hyperactivity in young adult mice (Skorput et al. 2015; Skorput and Yeh 2016).

In contrast to the relatively small contingent of cortical GABAergic interneurons, the glutamatergic pyramidal neurons constitute approximately 70–80% of cortical neurons and provide the sole output to subcortical and contralateral cortical regions (DeFelipe and Fariñas 1992). They are born intracortically in the proliferative zones along the dorsal rim of the telencephalic vesicles (Parnavelas 2000). During radial migration, radial glial cells (RGCs) in the ventricular zone divide asymmetrically to produce intermediate progenitor cells (IPCs; Mione et al. 1997; Noctor et al. 2004). The IPCs in the subventricular zone divide to produce postmitotic neurons that migrate through the intermediate zone and subplate, assemble in an inside-out fashion to establish the cortical plate, and eventually form the 6-layered cortex (Angevine and Sidman 1961; Rakic 1974; Marín-Padilla 1978; Nadarajah and Parnavelas 2002; Kriegstein and Noctor 2004; Noctor et al. 2004; Kriegstein and Alvarez-Buylla 2009). While earlier studies uncovered many effects of prenatal ethanol exposure on the migration and proliferation of cortical pyramidal neurons (Miller 1986) and their morphology (Hammer and Scheibel 1981; Lopez-Tejero et al. 1986; Miller 1988; Miller et al. 1990), additional information is needed to fully comprehend the impact of the ethanol-induced aberrances on cortical form and function.

Impaired learning and attention, emotional regulation, fine-motor skills as well as hyperactivity and impulsivity have all been associated with FASD (Streissguth et al. 1991; Mattson and Riley 1998; Mattson et al. 1998; Riley and McGee 2005; Franklin et al. 2008; Jirikowic et al. 2008; Carr et al. 2010). Disrupted sensory processing, mediated centrally by the somatosensory cortex (Amaral 2013), underlies many of these cognitive and behavioral deficits (Franklin et al. 2008; Jirikowic et al. 2008; Carr et al. 2010). For this reason, we focused investigation of the effects of *in utero* ethanol exposure on the developing somatosensory cortex. We hypothesized that an episode of *in utero* binge-type ethanol exposure, targeting a critical time in the migration of cortical neurons, would disrupt radial migration, and have enduring consequences on the form and function of pyramidal neurons in the somatosensory cortex. We report that *in utero* ethanol exposure results in an aberrant pattern of radial migration. In addition, we uncovered altered morphology and synaptic activity of layer V/VI pyramidal neurons in the early postnatal period and changes in tactile sensitivity in young adolescent mice exposed prenatally to ethanol. This speaks to *in utero* ethanol exposure exerting a persistent effect that impacts synaptogenesis and formation of neural circuits in the developing somatosensory cortex.

Materials and Methods

Animals

All animal procedures were approved by the Dartmouth Institutional Animal Care and Use Committee and are in strict compliance with NIH guidelines and Federal regulations. This study used male and female C57BL/6 wild-type embryos and mice and Thy1-YFP mice (B6.Cg-Tg(Thy1-YFP)16Jrs/J; Jackson Labs, stock #003 709; Feng et al. 2000). For timed-pregnancy, male and female mice were housed overnight and separated the following day. This day was designated as the day of conception, or embryonic day (E) 0.5. Female mice were weighed daily and pregnant female mice were identified by consistent weight gain. The day of birth was designated as postnatal day (P) 0.5. Animals were housed on a 12-h light–dark cycle.

PCR-Based Sex Genotyping

The tails were collected for genotyping to determine the sex of each embryo. We adopted a standard PCR protocol (Stratman et al. 2003) using primers for the male-specific sex determining region Y (SRY), which is found exclusively on the Y chromorosome.

SRY forward primer: TTG TCT AGA GAG CAT GGA GGG CCA TGT CAA

SRY reverse primer: CCA CTC CTC TGT GAC ACT TTA GCC CTC CGA

(http://mgc.wustl.edu/protocols/pcr_genotyping_primer_pairs)

Binge-Type Ethanol Exposure Paradigm

Prior to ethanol exposure, all animals were maintained on standard lab chow (Research Diets) with water available *ad libitum*. Timed-pregnant dams were acclimated to the Lieber–DeCarli liquid diet (Lieber and DeCarli 1989) on E12.5 and then randomly assigned to control or experimental groups at E13.5. Individually housed pregnant dams were administered a liquid diet containing 5% ethanol (w/w) or an isocaloric control containing maltose from E13.5 through E16.5, spanning a critical period in radial migration (Fig. 1A; Clancy et al. 2001). For all groups, the food was replenished every 24 h, and water was available *ad libitum*. Pregnant dams were weighed and food

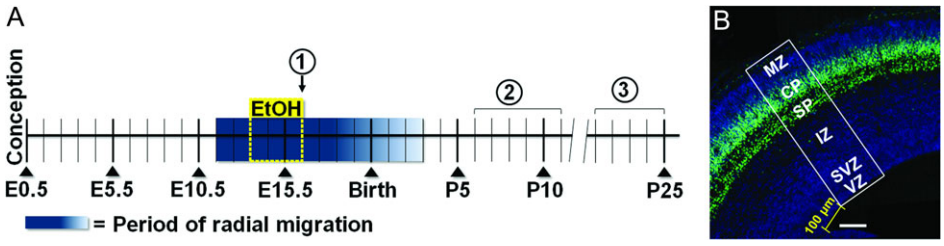

Figure 1. Experimental timeline and region of interest for analyzing E16.5 coronal sections. *A*: Graded blue box highlights the period of radial migration, beginning at ~E11.5 and tapering out by ~P3. Binge-type ethanol exposure begins on E13.5 and ends on E16.5 (yellow dashed lines). Encircled numbers above the timeline denote experimental time points: (1) Assessment of radial migration and cell proliferation at E16.5; (2) Measurement of spontaneous GABA- and glutamate-mediated synaptic activity in layer II/III and layer V/VI pyramidal neurons in the P6–P11 somatosensory cortex; (3) Adhesive tape removal test from P21–P25. *B*: A 200-µm wide bin positioned 100 µm from the cortical striatal juncture and spanning the entire thickness of the cortex was defined as the region of interest (ROI) in E16.5 coronal sections. Ventricular zone (VZ), subventricular zone (SVZ), intermediate zone (IZ), subplate (SP), cortical plate (CP), marginal zone (MZ). Scale bar = 100 µm.

consumption was recorded daily. Immediately following the binge-type ethanol exposure period, all animals were returned to standard lab chow. This model resulted in dam blood alcohol levels of 80 ± 21 mg/dL measured at 4.5 h into the dark cycle on E15.5 and did not affect litter size (Skorput et al. 2015).

Immunohistochemical Processing of Embryonic Brain Tissue

Procedure

On E16.5, pregnant dams were asphyxiated with CO_2 and the embryos removed by C-section. Embryonic brains were dissected, immerse fixed in 4% paraformaldehyde (PFA)/0.1 M PBS overnight at 4 °C and cryoprotected in 30% sucrose/0.1 M PBS. Thirty-micron coronal cryosections were cut using a sliding microtome. Immunohistochemistry was performed on 10 consecutive cryosections per brain, with the first section collected using the initial presentation of the cortical hem as an anatomical landmark. Sections were incubated in 0.1% BSA/0.25% Triton X-100/0.1 M PBS for 20 min, blocked in 10% normal goat serum (NGS)/0.25% Triton X-100/0.1 M PBS for 30 min, incubated in primary antibody/0.25% Triton X-100/0.1 M PBS for 48 h at 4 °C, and then in the appropriate Alexa-Fluor® secondary antibody/0.1 M PBS overnight at 4 °C. Sections were then incubated overnight in 0.1 M PBS at 4 °C, mounted, counterstained with 4′,6-diamidino-2-phenylindole (DAPI), and coverslipped with FluorSave Reagent (Calbiochem). Primary antibodies include: rabbit antiTbr2 (1:2000; gift from Dr. R. Hevner; see Englund et al. 2005), rabbit antiTbr1 (1:2750; gift from Dr R. Hevner; see Englund et al. 2005), mouse antiPax6 (1:10; DSHB), rabbit-antiCux1 (1:250; Santa Cruz) and mouse antiKi67 (Novocastra™). Secondary antibodies include: goat antirabbit 488 (1:1000; Molecular Probes), goat antimouse 555 (1:1000; Molecular Probes), and goat antimouse 488 (1:1000; Molecular Probes). Histological sections processed in parallel without the primary antibody served as negative control and were included for all experiments.

Immunofluorescent images were obtained using a spinning disk confocal upright microscope (BX61WI; Olympus, Center Valley, PA) with a CCD camera (Hamamatsu). A 10 × 0.30 NA objective (Olympus) was used to visualize fluorescent profiles. IPLab version 4.0 software (BD Bioscience) was used to capture digitized images, which were montaged using Fiji (Image J; Preibisch et al. 2009; Schindelin et al. 2012; Schneider et al. 2012).

Analysis

The region of interest (ROI) was defined by a 200-μm wide bin across the entire thickness of the embryonic somatosensory cortex, 100 μm distal from the corticostriatal juncture (Fig. 1*B*). Intensity of immunofluorescence, determined by using the plot profile application of FIJI (Image J) (Schindelin et al. 2012; Schneider et al. 2012) and based on the ratio of change in immunofluorescence to baseline ($\Delta F/F_{Baseline}$), was measured across the total thickness of the cortex within the ROI and analyzed for individual cortical zones. Cortical zones were defined by DAPI counterstaining in the same histological sections processed for immunohistochemistry. In constructing immunofluorescence distribution histograms (Fig. 2*C*, *F*, *I*, *L*), each cortical zone was divided into 10 bins of equal width, which provided sufficient data points to determine the distribution of immunofluorescence intensity in any given zone. The average immunofluorescence intensity calculated for each bin was then plotted as a function of the corresponding bin. Values derived from analyzing the immunofluorescence intensity of Pax6/Tbr2/Ki67, Tbr1, and Cux1 immunofluorescence were normalized to the average of that in the cortical plate, ventricular zone, or marginal zone, respectively. The average Ki67 immunofluorescence intensity was calculated and plotted for each cortical zone. All analyses were performed blinded to treatment condition.

Immunohistochemical Processing of Postnatal Brain Tissue

Procedure

Postnatal Day 7 control and ethanol-exposed wild-type and Thy1-YFP mice were transcardially perfused with 4% PFA/0.1 M, the brains dissected, and immerse fixed overnight in 4% PFA/0.1 M at 4 °C. The brains were then cryoprotected overnight in 15% sucrose/0.1 M PBS at 4 °C, transferred to a 30% sucrose/0.1 M PBS solution and stored at 4 °C. Thirty-micron coronal cryosections were cut using a sliding microtome, and 13 serial sections were processed, beginning at the first presentation of the hippocampus. For Cux1 immunostaining of wild-type somatosensory cortex, histological sections were incubated in 0.1% BSA/0.5% Triton X-100/0.1 M PBS, blocked in 10% NGS/0.5% Triton X-100/0.1 M PBS, incubated in rabbit-antiCux1 (1:250; Santa Cruz)/0.5% Triton X-100/0.1 M PBS for 24 h at 4 °C, and then in goat antirabbit 555 secondary antibody (1:1000; Molecular Probes) at 4 °C overnight. Sections were then washed in 0.1 M PBS, mounted, counterstained with DAPI, and coverslipped with FluorSave Reagent (Calbiochem). Negative control with primary antibody omitted was routinely processed in parallel. Thirty-micron coronal cryosections of somatosensory cortex from control and prenatal ethanol-exposed Thy1-YFP mice were mounted, counterstained with DAPI, and coverslipped with FluorSave Reagent (Calbiochem).

Analysis

Immunofluorescent images were obtained as previously described for embryonic cryosections, with the exception that cellSens software (Olympus, Center Valley, PA) was used to capture digitized images. The ROI was defined by a 500-μm wide bin across the entire thickness of the somatosensory cortex, 100 μm distal from the corticostriatal juncture. Cells were counted manually using the cell counter application in FIJI (Schindelin et al. 2012; Schneider et al. 2012) and cell density was calculated. All analyses were performed blinded to treatment condition.

5-Bromo-2′-Deoxyuridine (BrdU) Pulse-Chase Labeling

A BrdU pulse-chase assay was performed in conjunction with analysis of Ki67 immunoreactivity to assess the effects of *in utero* exposure to ethanol on cell proliferation. Time pregnant dams received one injection of 100 mg/kg of BrdU on E13.5. Embryonic brains were collected on E16.5, immerse fixed in 4% PFA/0.1 M PBS overnight at 4 °C, and cryoprotected in 30% sucrose/0.1 M PBS. Thirty-micron embryonic coronal cryosections were incubated in HCl for 45 min, followed by 30 min in borate buffer. Immunohistochemistry was performed using mouse anti-BrdU (1:10; DSHB) primary antibody. Immunofluorescent images were captured and the ROI was defined, both as previously described. Cells were counted manually using the cell counter application in FIJI (Schindelin et al. 2012; Schneider et al. 2012).

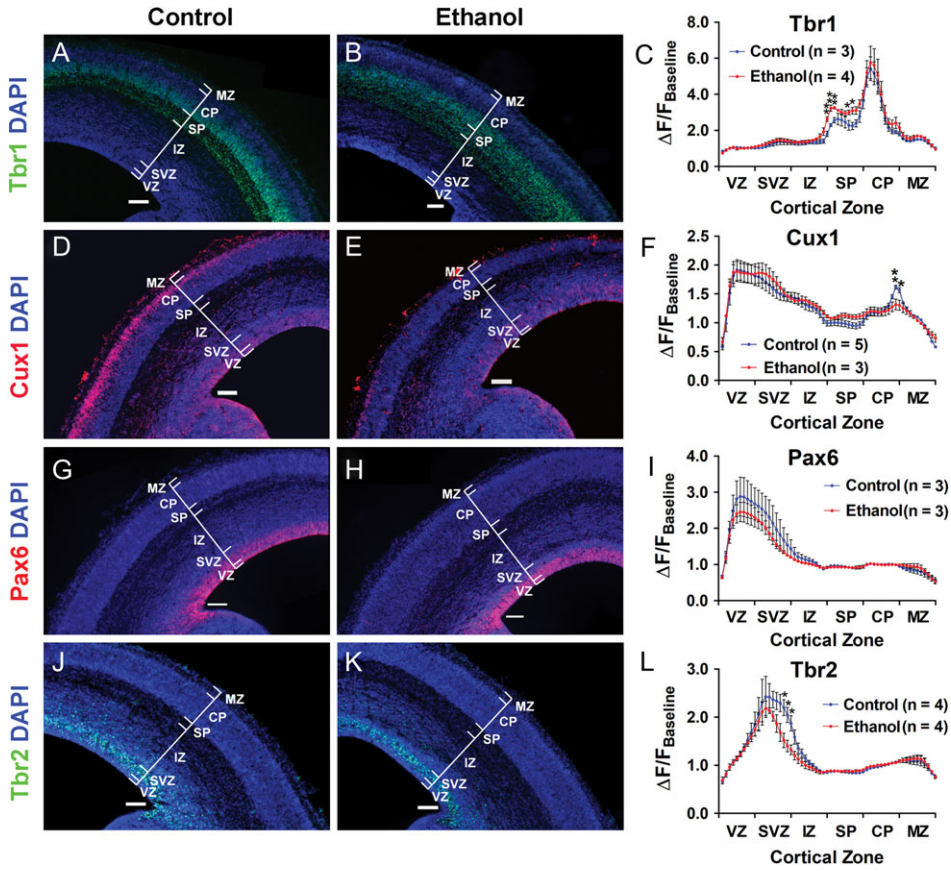

Figure 2. *In utero* binge-type ethanol exposure disrupts the radial migration of postmitotic pyramidal neurons. DAPI-counterstained coronal sections from E16.5 control and ethanol-exposed mouse somatosensory cortex stained for Tbr1 (*A*: control; *B*: ethanol), Cux1 (*D*: control; *E*: ethanol), Pax6 (*G*: control; *H*: ethanol), and Tbr2 (*J*: control; *K*: ethanol). *C*, *F*, *I*, *L*: Distribution histograms of immunofluorescence intensity measured across the total thickness of the cortex, normalized and stratified by cortical zones. Brackets delineate cortical zones in each representative section. Ventricular zone (VZ), subventricular zone (SVZ), intermediate zone (IZ), subplate (SP), cortical plate (CP), marginal zone (MZ). *n* Values included in the distribution histograms denote number of litters. Scale bar = 100 μm. $^{**}P < 0.01$, $^{*}P < 0.05$; An unpaired *t*-test was used to compare the means between control and ethanol-exposed cohorts for each individual bin. Data presented as mean ± SEM. See Supplementary Tables 1, 2, 4, 5 for exact *P*-values.

The cell density was then determined for each cortical zone. All analyses were performed blinded to treatment condition.

Electrophysiology

Acute slices containing the somatosensory cortex were prepared for whole-cell patch-clamp recording of cortical pyramidal neurons as previously described (Skorput et al. 2015). Briefly, P6-11 pups were asphyxiated with CO_2 and the brains were submerged in ice-cold oxygenated (95% O_2/5% CO_2) cutting solution containing (in mM): 3 KCl, 7 $MgCl_2$, 1.25 NaH_2PO_4, 0.5 $CaCl_2$, 28 $NaHCO_3$, 5 D-glucose, 110 sucrose, pH 7.4 (adjusted with 1 N NaOH). Coronal slices (200 μm) were cut using a vibrating microtome (Electron Microscopy Sciences) and placed in a recovery chamber for 30 min filled with 32 °C oxygenated (95% O_2/5% CO_2) artificial cerebrospinal fluid (aCSF) containing (in mM): 125 NaCl, 2.5 KCl, 1 $MgCl_2$, 1.25 NaH_2PO_4, 2 $CaCl_2{\cdot}2H_2O$, 25 $NaHCO_3$, 25 D-glucose, pH 7.4 (adjusted with 1 N NaOH). Slices were then transferred to room temperature aCSF for approximately 1 h prior to recording.

Borosilicate glass patch electrodes (Sutter Instrument; OD:1.5 mm; ID 0.86 mm) were pulled using a Flaming Brown Micropipette Puller (Sutter Instrument Model P80 PC) with a resistance of 6–8 MΩ measured in external solution. Electrodes were filled with a K-gluconate-based internal solution containing (in mM): 100 K-gluconate, 2 $MgCl_2$, 1 $CaCl_2$, 11 EGTA, 10 HEPES, 30 KCl, 3 Mg^{+2} ATP, 3 Na^{+} GTP, adjusted to pH 7.3 with 1 N KOH. Multi-barrel drug pipettes, pulled using a vertical Micro Electrode Puller (Stoelting Co. Cat. No. 51 217), consisted of a center barrel (Sutter Instrument; OD:1.2 mm; ID 0.69 mm) and 5 surrounding outer barrels (Sutter Instrument; OD:1.5 mm; ID 0.86 mm).

A brain slice was transferred to a custom-made acrylic recording chamber secured to a fixed-stage upright fluorescence microscope (Olympus BX51 WI) equipped with Hoffman Modulation Contrast optics. Slices were perfused with oxygenated aCSF (0.5–1.0 mL/min) and maintained at 32 °C. Whole-cell recordings were performed using an AxoPatch 200 A amplifier (Axon Instruments) and membrane currents were recorded with low-pass filtering at 5 kHz (Clampex version 9.0, Molecular Devices) and digitized at 20 kHz (Digidata 1320 A; Molecular Devices).

All synaptic currents were recorded at a holding potential of −65 mV. Figure 5A shows a recording pipette (black solid line) patched onto a layer V/VI pyramidal neuron and a multi-barrel drug pipette (dotted black line) placed approximately 20 μm from the cell body. Separate channels of a Multichannel Picospritzer (General Valve Corporation) were connected to

specific barrels of the drug pipette to enable separate pressure ejection (<3 psi) of 20 μM APV/20 μM CNQX to isolate GABA-mediated postsynaptic currents ($GABA_{PSCs}$), 20 μM bicuculline to isolate glutamate-mediated postsynaptic currents (Glu_{PSCs}), or aCSF, to monitor baseline spontaneous synaptic activity. For each cell, baseline spontaneous synaptic activity was monitored first for 2 min, followed by a 2-min recording of either pharmacologically isolated $GABA_{PSCs}$ or Glu_{PSCs}, and a 2-min washout period with aCSF. This protocol was repeated for the other pharmacological blocker such that both $GABA_{PSCs}$ and Glu_{PSCs} were assessed in random order in the same cell. MiniAnalysis software (Version 6.0; Synaptosoft) was used to analyze the frequency and amplitude of $GABA_{PSCs}$ and Glu_{PSCs} during the 2-min recording epoch. Only cells that exhibited both Glu_{PSCs} and $GABA_{PSCs}$ were included for analysis of $Glu_{PSCs}/GABA_{PSCs}$ ratio. All analysis was conducted blind to treatment.

Pyramidal Cell Filling and Reconstruction

Pyramidal cells were filled intracellularly during whole-cell recording by including 2% neurobiotin (Vector Laboratories) in the K-gluconate internal recording solution (Fig. 5A–C). After recording, slices were fixed in 4% PFA/0.1 M overnight at 4 °C, cryoprotected in 30% sucrose/0.1 M PBS, and stored at 4 °C. To visualize the neurobiotin-filled cells, slices were first washed in 0.1 M PBS prior to incubation in 3% H_2O_2/0.1 M PBS for 30 min. Following a 10-min rinse in 0.1 M PBS, the slices were incubated for an additional 30 min in 3% H_2O_2/0.1 M PBS. After rinsing in 0.1 M PBS, the slices were blocked in 10% NGS/0.1 M PBS/0.4% Triton X-100/0.1 M PBS for 2 h at room temperature and then incubated in 10 μg/mL DyLight 594 Streptavidin (Vector Labs) overnight at 4 °C. Slices were then washed in 0.1 M PBS overnight, mounted, counterstained with DAPI, and coverslipped with FluorSave Reagent (Calbiochem). Z-stacked images of cells were acquired on a Zeiss LSM 510 laser-scanning confocal microscope with a HENE 543 Laser using a plan-apochromat 10×/0.45 NA objective, 1× zoom, at 2048 × 2048, with x,y,z at 0.44×0.44×3.0 μm. The cells were traced using Neurolucida 360 (MBF Bioscience, Williston, VT), followed by Sholl analysis and measurement of apical dendritic length and soma size.

Sholl Analysis

A modified version of the Sholl analysis (Sholl 1953) was employed in the present study using Neurolucida Explorer (MBF Bioscience, Williston, VT). Briefly, the center of a template of concentric circles with the radius set at 10-μm increments was placed over the soma of a reconstructed pyramidal neuron (Fig. 5B,C). For both apical and basal dendrites, raw values of dendritic complexity were derived based on the number of branch intersections per 10 μm radial increment. For complexity of basal dendrites, these raw values were used for comparison between the control and ethanol-exposed groups. However, the raw values could not be used to assess the complexity of apical dendrites because the apical dendritic shafts varied in length such that within-cohort averaging would have obscured the bimodal distribution of the apical tufts and the branching pattern of the proximal dendrites (e.g., Figs 5D and 7A). Therefore, for the apical dendrites, the number of intersections was analyzed per 10% and 5% of the total apical dendrite length for layers II/III and V/VI pyramidal neurons, respectively. All analysis was conducted blind to treatment.

Adhesive Tape Test

The adhesive tape test was adapted from Bouet et al. (Bouet et al. 2009) and assessed in P21–P25 control and ethanol-exposed young adolescent mice. Briefly, a mouse was placed into an empty cage and, following a 60-s acclimation period, a piece of tape large enough to cover the palm but not the toes of the mouse (~4 × 6 mm), was placed on the right and left forepaws (Fig. 8A). The mouse was then placed back into the empty cage and monitored for (1) the latency to their initial contact with the tape (when grooming was first observed) and (2) the length of time until both pieces of tape were removed (Fig. 8B). Only mice that removed both pieces of tape were included for analysis of removal time. Each trial lasted for a maximum of 120 s. The mice completed one trial for 5 consecutive days, at approximately the same time each day. All trials were conducted blind to treatment. Between 4 and 5 mice were used per litter, which included both males and females. All experiments were video recorded and were conducted in a clear plastic cage without any bedding, which was placed in the same location each day. The cage was cleaned between mice with Clidox® (1:18 dilution of Chlorine Dioxide in water, Dartmouth Center for Comparative Medicine and Research).

Experimental Design and Statistical Analysis

For histological analyses, sample size (n) represents the number of litters to minimize litter effects. A minimum of 3 litters were used per experiment, and between 1 and 3 brains were used per litter, consisting of a mix of male and female samples for each experiment. Ten 30-μm coronal serial sections, beginning at the first presentation of the cortical hem, were analyzed per embryonic brain. Thirteen 30-μm coronal serial sections, beginning at the first presentation of the hippocampus, were analyzed per postnatal brain. For behavioral studies, *n* also represents the number of litters.

For pyramidal cell morphological and electrophysiological data, *n* represents the number of cells. An average of 10 litters were used per treatment/age cohort and between 1 and 3 brains were used per litter. Recordings were obtained from between 1 and 3 acute slices containing the somatosensory cortex per brain, and an average of eight cells were recorded per litter.

All statistical analyses were conducted in GraphPad Prism (Version 5.0). For Sholl analysis data, a repeated measures 2-way ANOVA with Bonferroni post hoc test, was used with treatment (control or ethanol) and distance from the soma as factors. Distance from the soma was always significant ($P < 0.0001$) and there was never a significant interaction between factors ($P > 0.05$); therefore, we provide *P*-values only for treatment (see *Results*). For analysis of behavioral studies, a repeated measures 2-way ANOVA with Bonferroni post hoc test, was used with treatment (control or ethanol) and day as factors. Day as a factor was always significant ($P < 0.05$) and there was never a significant interaction between factors ($P > 0.05$); therefore, we provide *P*-values only for treatment (see *Results*). A Mann–Whitney *U* test was used to analyze the electrophysiological data since the data sets were non-normally distributed. For all other analyses, the average mean was compared between control and ethanol-exposed groups using an unpaired *t*-test, as indicated. All data are reported as mean ± SEM. Statistical power was determined based on sample sizes used in previous experiments with a similar design (Skorput et al. 2015) and by using G*Power (Version 3.1.9.2, Franz Faul, Universität Kiel, Germany, 1992–2014).

Results

In Utero Exposure to Binge-Type Ethanol Disrupts the Radial Migration of Postmitotic Pyramidal Neurons in the Embryonic Somatosensory Cortex

The timeframe of the inside-out incorporation of pyramidal cells into the cortical plate during corticogenesis (Angevine and Sidman 1961; Custo Greig et al. 2013) places our *in utero* binge-type ethanol exposure within the temporal window of active radial migration (E13.5–E16.5; graded blue box in Fig. 1*A*; Clancy et al. 2001). Using this model, we asked whether *in utero* binge-type ethanol exposure affected the expression of transcription factors that define the developmental progression of RGC-derived neuroprogenitor cells to early-born postmitotic pyramidal neurons in the embryonic somatosensory cortex.

We took advantage of the sequential expression of Pax6, Tbr2, and Tbr1 during corticogenesis (Englund et al. 2005). The homeodomain transcription factor, Pax6, is highly expressed in RGCs in the ventricular zone (Götz et al. 1998; Englund et al. 2005). Asymmetric division and generation of IPCs is marked by downregulation of Pax6 and upregulation of Tbr2, a T-domain transcription factor (Englund et al. 2005). The region of Tbr2 expression ranges from the basal ventricular zone to the lower intermediate zone, with a peak of expression in the subventricular zone (Englund et al. 2005). Subsequent differentiation into postmitotic pyramidal neurons is hallmarked by downregulation of Tbr2 and upregulation of Tbr1, another T-domain transcription factor (Englund et al. 2005). Expression of Tbr1 spans the upper intermediate to the marginal zone, with prominent expression in the cortical plate (Hevner et al. 2001; Englund et al. 2005).

Figure 2*A*,*B* illustrate Tbr1 expression in histological sections taken at equivalent levels from E16.5 control and age-matched ethanol-exposed somatosensory cortex, respectively. Data analyzed from such sections were used to construct the distribution histogram in Figure 2*C*, which plots the intensity of Tbr1 immunofluorescence ($\Delta F/F_{Baseline}$) as a function of cortical zones present at E16.5 under control or ethanol-exposed conditions. The Tbr1 immunofluorescence distribution histogram derived from the control cohort (Fig. 2*C*, blue line) featured 2 distinct peaks, each representing a band of concentrated Tbr1 immunofluorescence, one in the lower half of the subplate and the other in the lower half of the cortical plate; this pattern confirmed previous reports of Tbr1 expression (Hevner et al. 2001, Englund et al. 2005). By contrast, in the ethanol-exposed cohort (Fig. 2*C*, red line), Tbr1 immunofluorescence was diffusely distributed and scattered across the subplate and into the lower half of the cortical plate (Fig. 2*B*), effectively diluting the concentrated band of Tbr1 immunofluorescence seen in the subplate of control embryonic somatosensory cortex (Fig. 2*A*). Quantitative analysis of Tbr1 immunofluorescence revealed that the prominent peak of immunofluorescence in the subplate seen in the control somatosensory cortex was no longer evident following the binge-type ethanol exposure (Fig. 2*B*,*C*; subplate [Control: 2.585 ± 0.250 $\Delta F/F_{Baseline}$; ethanol: 3.221 ± 0.078 $\Delta F/F_{Baseline}$; $t(5) = 2.789$, $P = 0.0385$, unpaired *t*-test]; see Supplementary Table 1 for full quantitative analysis of Fig. 2*C*). Taken together, these results point to disrupted radial migration of early-born pyramidal neurons.

Later-born pyramidal neurons also displayed an aberrant pattern of radial migration. During embryonic corticogenesis, nuclear expression of the transcription factor Cux1 is highest in the upper portion of the cortical plate but can also be seen throughout the subventricular zone and intermediate zone; thus, Cux1 marks radially migrating pyramidal neurons destined for layers II/III (Nieto et al. 2004). Figure 2*D* illustrates a distinct and intense band of Cux1 immunofluorescence in the upper cortical plate of control E16.5 somatosensory cortex, corresponding to the peak in the immunofluorescence distribution histogram in Figure 2*F*. Remarkably, this band of concentrated Cux1 immunofluorescence was absent in the cortical plate of sections from E16.5 ethanol-exposed somatosensory cortex (Fig. 2*E*), and Cux1 immunofluorescence intensity was significantly lower compared to control (Fig. 2*F*; Upper half of cortical plate [Control: 1.431 ± 0.024 $\Delta F/F_{Baseline}$; ethanol: 1.262 ± 0.082 $\Delta F/F_{Baseline}$: $t(6) = 2.480$, $P = 0.0478$, unpaired *t*-test]). No significant differences were found for Cux1 expression in the remaining cortical zones of control versus ethanol-exposed somatosensory cortex. Detailed quantitative analysis for Figure 2*F* is presented in Supplementary Table 2.

Potential sex-dependent differences in Cux1 expression were also analyzed. There was no difference in Cux1 immunofluorescence intensity between males and females for either the control or ethanol cohorts (Supplementary Fig. 1; see Supplementary Table 3 for full statistics). Sex-dependent differences were not systematically analyzed for Tbr1, Tbr2, and Pax6 expression. However, since we are not aware of hormonal influences that target transcription factors early in embryonic development, we postulated that the absence of sex-associated differences in Cux1 expression is applicable to the other transcriptional markers examined at E16.5 in the present study. Therefore, Figure 2 illustrates data that were pooled from histological sections of male and female somatosensory cortex.

In addition to the $Tbr1^+$ and $Cux1^+$ postmitotic neuronal populations, we investigated potential ethanol-induced changes in neuroprogenitor cells by assessing the expression patterns of Pax6 and Tbr2. We found no differences in Pax6 expression between the control (Fig. 2*G*) and ethanol-exposed cohorts (Fig. 2*H*), as expression peaked in the ventricular zone for both (Fig. 2*I*; see Supplementary Table 4 for full statistics). Similarly, for the pattern of Tbr2 expression, fluorescence intensity peaked in the subventricular zone for both control (Fig. 2*J*) and ethanol-exposed somatosensory cortices (Fig. 2*K*,*L*; see Supplementary Table 5 for full statistics). These data suggest that *in utero* ethanol exposure does not significantly affect neuroprogenitor cells, although we found a decrease in Tbr2 immunofluorescence in the ethanol-exposed compared to control cohorts immediately after the peak in the subventricular zone (Fig. 2*L*). Taken together, the aberrant distribution of Tbr1 immunofluorescence in the subplate and that of Cux1 in the cortical plate suggests that *in utero* ethanol exposure either delayed migration or disrupted their temporal pattern of expression.

In Utero Exposure to Binge-Type Ethanol Does Not Affect Neuronal Proliferation in the Embryonic Somatosensory Cortex

A BrdU pulse-chase assay was performed to assess whether cell proliferation was affected during the period of *in utero* binge-type ethanol exposure. At E16.5, there were no significant differences in the density of $BrdU^+$ cells stratified by cortical zone between the control and ethanol-exposed cohorts (Fig. 3*A*–*C*). Figure 3*A*,*B* also illustrate qualitatively comparable cortical zones between the control and ethanol-exposed somatosensory cortex (quantitative data not shown). Therefore, the width of cortical zones did not affect density measurements.

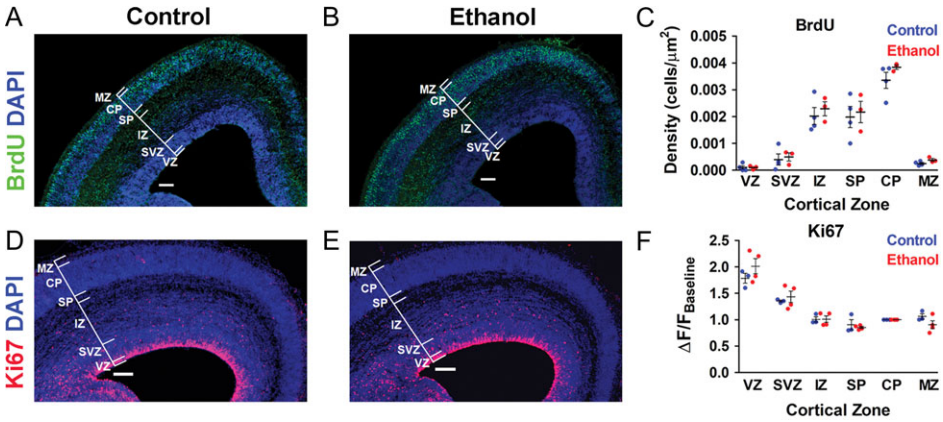

Figure 3. Cell proliferation in the embryonic somatosensory cortex is not affected during the period of binge-type ethanol exposure *in utero*. *A*, *B*: Coronal sections from E16.5 control (*A*) and ethanol-exposed (*B*) mouse somatosensory cortex immunostained for BrdU and counterstained for DAPI. *C*: Density of $BrdU^+$ cells stratified by cortical zone. *D*, *E*: DAPI-counterstained coronal sections from E16.5 control (*D*) and ethanol-exposed (*E*) mouse somatosensory cortex immunostained for Ki67. *F*: Normalized immunofluorescence intensity across the total cortical thickness, stratified by cortical zone. Brackets delineate cortical zones in each representative section. Ventricular zone (VZ), subventricular zone (SVZ), intermediate zone (IZ), subplate (SP), cortical plate (CP), marginal zone (MZ). Control: (BrdU $n = 4$; Ki67 $n = 3$); Ethanol: (BrdU $n = 3$; Ki67 $n = 4$); $n =$ litters. Each dot represents data derived from one litter. Scale bar = 100 μm. Unpaired *t*-test revealed no significant differences in density of $BrdU^+$ cells (*C*) and Ki67 immunofluorescence intensity (*F*). VZ: (BrdU [Control: $1.0030 \times 10^{-4} \pm 6.8670 \times 10^{-5}$ cells/μm²; Ethanol: $9.8670 \times 10^{-5} \pm 3.9080 \times 10^{-5}$ cells/μm²; $t(5) = 0.0181$, $P = 0.9863$]; Ki67 [Control: 1.7837 ± 0.0934 $\Delta F/F_{Baseline}$; Ethanol: 2.0134 ± 0.1439 $\Delta F/F_{Baseline}$; $t(5) = 1.2270$, $P = 0.2746$]); SVZ: (BrdU [Control: $3.950 \times 10^{-4} \pm 2.060 \times 10^{-4}$ cells/μm²; Ethanol: $4.9330 \times 10^{-4} \pm 1.4930 \times 10^{-4}$ cells/μm²; $t(5) = 0.3592$, $P = 0.7341$]; Ki67 [Control: 1.3533 ± 0.0187 $\Delta F/F_{Baseline}$; Ethanol: 1.4341 ± 0.1095 $\Delta F/F_{Baseline}$; $t(5) = 0.6194$, $P = 0.5628$]); IZ: (BrdU [Control: $0.0020 \pm 3.1710 \times 10^{-4}$ cells/μm²; Ethanol: $0.0023 \pm 2.6030 \times 10^{-4}$ cells/μm²; $t(5) = 0.6289$, $P = 0.5570$]; Ki67 [Control: 1.0070 ± 0.0509 $\Delta F/F_{Baseline}$; Ethanol: 1.0119 ± 0.0615 $\Delta F/F_{Baseline}$; $t(5) = 0.0591$, $P = 0.9552$]); SP: (BrdU [Control: $0.0020 \pm 3.9390 \times 10^{-4}$ cells/μm²; Ethanol: $0.0022 \pm 3.9710 \times 10^{-4}$ cells/μm²; $t(5) = 0.3311$, $P = 0.7540$]; Ki67 [Control: 0.9046 ± 0.0995 $\Delta F/F_{Baseline}$; Ethanol: 0.8537 ± 0.0199 $\Delta F/F_{Baseline}$; $t(5) = 0.5882$, $P = 0.5819$]); CP: (BrdU [Control: $0.0034 \pm 3.0080 \times 10^{-4}$ cells/μm²; Ethanol: $0.0038 \pm 8.0350 \times 10^{-5}$ cells/μm²; $t(5) = 1.353$, $P = 0.2340$]; Ki67 [all values normalized to CP]); MZ: (BrdU [Control: $2.5000 \times 10^{-4} \pm 3.9040 \times 10^{-5}$ cells/μm²; Ethanol: $3.8300 \times 10^{-4} \pm 5.4560 \times 10^{-5}$ cells/μm²; $t(5) = 2.0480$, $P = 0.0959$]; Ki67 [Control: 1.0642 ± 0.0520 $\Delta F/F_{Baseline}$; Ethanol: 0.9056 ± 0.0756 $\Delta F/F_{Baseline}$; $t(5) = 1.5940$, $P = 0.1719$]).

BrdU labels cells during the Synthesis (S) phase of the cell cycle (Gratzner 1982). Thus, the population of cells labeled in our experiments represents those derived from S phase progenitors in the lower ventricular zone (RGCs) at the time of the BrdU injection on E13.5 that subsequently migrated into the developing cortex. As illustrated in Figure 3*C*, the majority of the $BrdU^+$ cells were found in the intermediate zone, subplate, and cortical plate by E16.5. However, the similarity in the pattern of BrdU expression does not rule out the possibility that ethanol could have affected proliferative cells in stages of the cell cycle other than the S phase. In this light, we examined the expression of Ki67 immunoreactivity as an endogenous marker of cells in all proliferative stages (Gap1, S, Gap2, and mitosis) and an important companion analysis to BrdU (Gerdes et al. 1984; Scholzen and Gerdes 2000; Kee et al. 2002; Nixon and Crews 2004; Oh et al. 2009; McClain et al. 2011).

The dense concentration of $Ki67^+$ cells in the ventricular zone of E16.5 coronal sections (Fig. 3*D*,*E*) precluded the identification of individual neurons, as was possible for the $BrdU^+$ cells (Fig. 3*A*,*B*). Therefore, the average fluorescence intensity per cortical zone was assessed and normalized to that of the cortical plate, which displayed low Ki67 expression. Similar to BrdU, there were no significant differences in Ki67 expression in control and ethanol-exposed embryos at E16.5 (Fig. 3*D*–*F*). The combined results of the BrdU and Ki67 experiments suggest that binge-type ethanol exposure from E13.5–E16.5 does not affect proliferation of pyramidal neurons.

Postnatal Day 6–8 Mice Exposed *In Utero* to Binge-Type Ethanol Exhibit Increased Spontaneous Activity and Altered Neuronal Morphology of Somatosensory Cortex Pyramidal Neurons

The early postnatal period in rodents is a time of active synaptogenesis and initial wiring of the cortical circuitry (Meller et al. 1968; Johnson and Armstrong-James 1970; Blue and Parnavelas 1983; Uylings et al. 1990). We analyzed spontaneous synaptic activity from P6 through P11 to determine if there were any differences due to *in utero* exposure to ethanol at an early stage of synapse formation. Data were analyzed separately for P6-8 and P9-11.

The incidence of spontaneous synaptic events was low in layer II/III and layer V/VI pyramidal neurons in P6-11 somatosensory cortex of both control and ethanol-exposed pups (Fig. 4*A*,*B*, *D*,*E*; Fig. 6*A*–*D*). This low incidence precluded analysis of action potential-independent postsynaptic activity. Concomitant application of APV, CNQX, and bicuculline abolished all spontaneous postsynaptic events (Fig. 4*C*). Therefore, GABA-mediated spontaneous postsynaptic current events ($GABA_{PSCs}$) were isolated in the presence of AMPA and NMDA receptor antagonists, CNQX and APV respectively, and glutamate-mediated spontaneous postsynaptic current events (Glu_{PSCs}) were isolated in the presence of bicuculline, a $GABA_A$ receptor antagonist. Given that GABA is paradoxically depolarizing early in development (Obata et al. 1978; Ben-Ari et al. 1989; Cherubini et al. 1991; Owens and Kriegstein 2002; reviewed in Ben-Ari 2002), and that this was not systematically assessed in the present study, we were mindful to use the terms "$GABA_{PSC}$" or "Glu_{PSC}" in lieu of the more conventional designation of "inhibitory" or "excitatory" postsynaptic currents, respectively.

In P6-8 layer V/VI pyramidal neurons, the frequency of spontaneous postsynaptic events was significantly increased in ethanol-exposed P6-8 somatosensory cortex compared to age-matched controls for both $GABA_{PSCs}$ (Fig. 4*D*; Control: 0.0322 ± 0.0053 Hz; ethanol: 0.0937 ± 0.0200 Hz; $P = 0.0045$, Mann–Whitney *U* test) and Glu_{PSCs} (Fig. 4*E*; control: 0.0063 ± 0.0016 Hz; ethanol: 0.0153 ± 0.0032 Hz; $P = 0.0223$, Mann–Whitney *U* test). However, there were no significant differences in the frequency of spontaneous events in layer II/III pyramidal neurons for either $GABA_{PSCs}$ (Fig. 4*D*; control: 0.0242 ± 0.0048 Hz; ethanol: 0.0272 ±

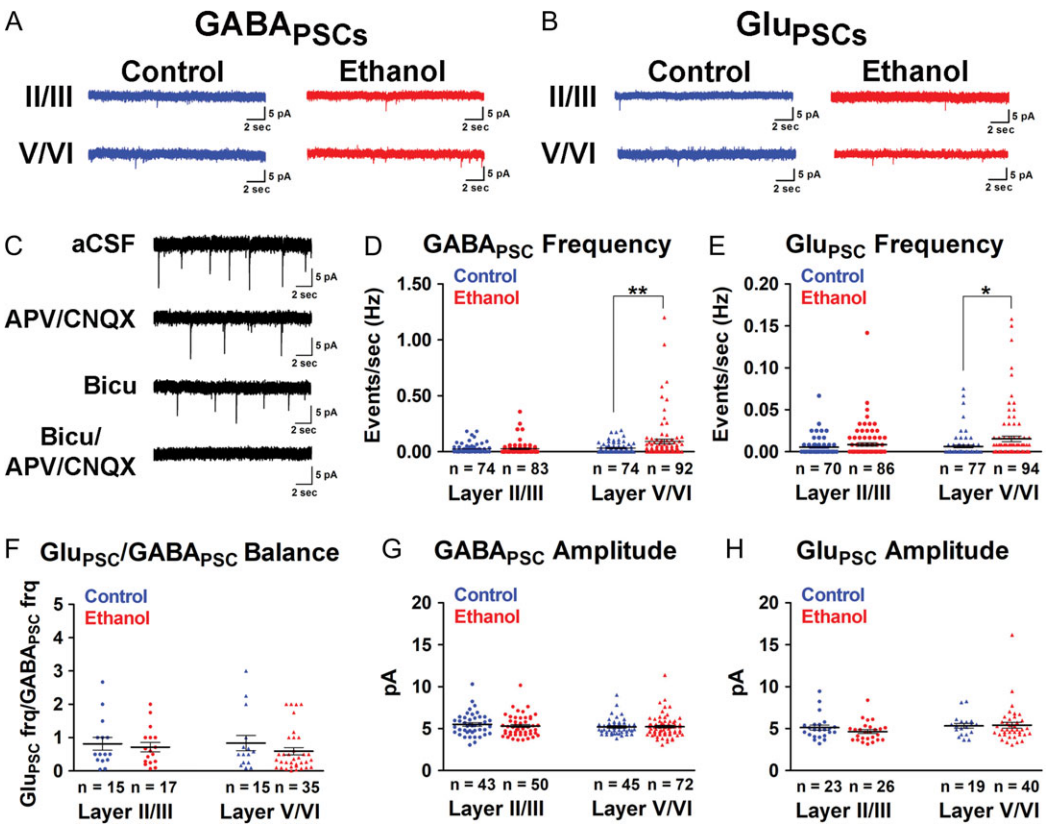

Figure 4. Binge-type ethanol exposure *in utero* increases spontaneous synaptic activity in P6-8 layer V/VI somatosensory cortex pyramidal neurons. *A*, *B*: $GABA_{PSCs}$ (*A*) and Glu_{PSCs} (*B*) were monitored in layer II/III and layer V/VI pyramidal neurons in control (blue traces) and ethanol-exposed (red traces) somatosensory cortical slices. *C*: Spontaneous synaptic activity was completely blocked by bicuculline/APV/CNQX. *D*, *E*: Mean frequency (Hz) of $GABA_{PSCs}$ (*D*) and Glu_{PSCs} (*E*) of layer II/III and layer V/VI pyramidal neurons in control (blue) and age-matched ethanol-exposed (red) cohorts. *F*: There was no net change in $Glu_{PSCs}/GABA_{PSCs}$ balance at P6-8. *G*, *H*: There were no significant differences in the amplitude of $GABA_{PSCs}$ (*G*) or Glu_{PSCs} (*H*) between control (blue) and ethanol-exposed (red) cohorts. *n* = number of cells. Each dot represents data derived from one pyramidal cell. $^{**}P < 0.01$, $^{*}P < 0.05$ (Mann–Whitney *U* test). Data presented as mean±SEM. See *Results* for exact *P*-values for *D*–*F*. See Supplementary Table 6 for exact *P*-values for *G*, *H*.

0.0062 Hz; $P = 0.7229$, Mann–Whitney *U* test) or Glu_{PSCs} (Fig. 4*E*; control: 0.0054 ± 0.0013 Hz; ethanol: 0.0086 ± 0.0021 Hz; $P = 0.7366$, Mann–Whitney *U* test). There were also no significant differences in the amplitude of events for superficial and deep layer pyramidal neurons (Fig. 4*G*,*H*; see Supplementary Table 6 for full statistics). This suggested that ethanol exerted its effects at the level of presynaptic inputs rather than postsynaptic GABAergic or glutamatergic receptors. There were no overall sex-associated differences in either frequency (Supplementary Fig. 2A–H; see Supplementary Table 7 for full statistics) or amplitude (data not shown) of spontaneous synaptic events in layer II/III or layer V/VI pyramidal neurons in either the control or ethanol-exposed cohort. Therefore, the data illustrated in Figure 4 includes those pooled from males and females.

The ratio of Glu_{PSCs} to $GABA_{PSCs}$ can be an early developmental indicator of an excitatory/inhibitory (E/I) imbalance later in life when glutamate and GABA mediate excitatory and inhibitory neurotransmission, respectively. As shown in Figure 4*F*, at P6-8, the observed increase in both Glu_{PSCs} and $GABA_{PSCs}$ resulted in no net change in the $Glu_{PSCs}/GABA_{PSCs}$ ratio for either layer II/III (control: 0.8161 ± 0.1914; ethanol: 0.7158 ± 0.1376; $P = 0.8795$, Mann–Whitney *U* test) or layer V/VI (control: 0.8373 ± 0.2264; ethanol: 0.5942 ± 0.1072; $P = 0.2705$, Mann–Whitney *U* test).

In addition to spontaneous synaptic activity, ethanol exposure *in utero* also affected the morphology of layer V/VI pyramidal neurons in the P6-8 somatosensory cortex. Sholl analysis revealed a significant decrease in dendritic complexity in the apical dendrite of the ethanol-exposed cohort (Fig. 5*D*; ($F(1, 1121) = 6.532$, $P = 0.0132$), repeated measures 2-way ANOVA, main effect of treatment). Bonferroni post hoc analysis of the 2-way ANOVA revealed that the observed decrease is statistically significant at 25% and 90% of the total apical dendritic length (25%—control: 9.500 ± 1.4307 intersections; ethanol: 5.6667 ± 0.7772 intersections; $P<0.05$; 90%—control: 13.0 ± 1.0419 intersections; Ethanol: 9.111 ± 0.9657 intersections; $P < 0.05$). The complexity of basal dendrites also decreased in the ethanol-exposed cohort (Fig. 5*E*; ($F(1, 708) = 5.344$, $P = 0.0243$), repeated measures 2-way ANOVA, main effect of treatment). Furthermore, the apical dendrite of layer V/VI pyramidal neurons was also significantly shorter in the ethanol-exposed cohort (Fig. 5*F*; control: 2085 ± 150.4 μm; ethanol: 1578 ± 134.9 μm; $t(59)=2.445$, $P=0.0175$, unpaired *t*-test).

In contrast, in layer II/III pyramidal neurons, there was no difference in apical dendritic complexity (Fig. 5*G*; ($F(1, 315) = 0.3296$, $P = 0.5696$) repeated measures 2-way ANOVA, main effect of treatment), basal dendritic complexity (Fig. 5*H*; ($F(1, 490) = 0.2890$, $P = 0.5943$) repeated measures 2-way ANOVA, main effect of treatment) or apical dendritic length (Fig. 5*F*; control: 733.6 ± 61.56 μm; ethanol: 694.4 ± 79.93 μm; $t(35) = 0.3938$, $P = 0.6961$, unpaired *t*-test). Soma size was not affected in either the deep or superficial layer pyramidal neurons (Fig. 5*I*; Layer II/

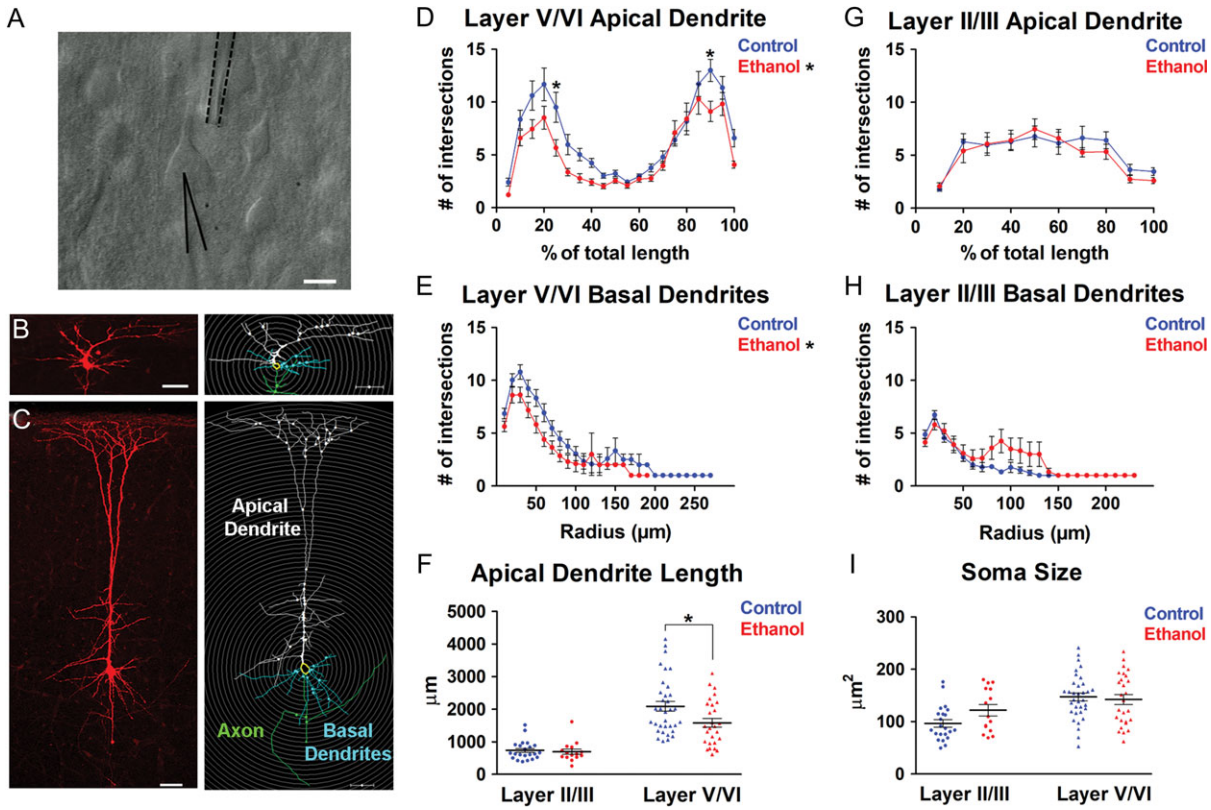

Figure 5. Binge-type *in utero* ethanol exposure altered the dendritic complexity of pyramidal neurons in the P6-8 somatosensory cortex. *A*: Acute brain slice containing the somatosensory cortex illustrating a layer V/VI pyramidal neuron (center) with a neurobiotin-filled patch-clamp recording electrode attached (solid black line) and multi-barrel drug pipette nearby (dotted black line). *B*, *C*: Neurobiotin-filled (left) and Neurolucida-reconstructed (right) Layer II/III (*B*) and Layer V/VI (*C*) pyramidal neuron in the somatosensory cortex. In reconstructed images, apical dendrites of pyramidal neurons are labeled white, soma yellow, basal dendrites blue, and axon green. Gray concentric circles for Sholl analysis were overlaid at 10 µm intervals. Sholl analysis of layer V/VI pyramidal neuron apical dendrite (*D*) and basal dendrites (*E*) and layer II/III pyramidal neuron apical dendrite (*G*) and basal dendrites (*H*) in control (blue lines) and ethanol-exposed (red lines) somatosensory cortex. Mean apical dendritic length (*F*) and soma size (*I*) in control (blue) and ethanol-exposed (red) layer II/III and layer V/VI pyramidal neurons. Layer II/III: (control: $n = 22$; ethanol: $n = 15$); Layer V/VI: (control: $n = 34$; ethanol: $n = 27$); n = number of cells. Each dot in (*F*) and (*I*) represents data derived from one pyramidal cell. Scale bar (*A*) = 10 µm. Scale bars (*B*, *C*) = 50 µm. *D*, *E*: $^*P < 0.05$ (significant main effect of treatment, repeated measures 2-way ANOVA); *D*, $^*P < 0.05$ (Bonferroni post hoc analysis); *F*, $^*P < 0.05$ (unpaired *t*-test). *D*, *E*, *G*, *H*: Repeated measures 2-way ANOVA with Bonferroni post hoc test; *F*, *I*: unpaired *t*-test. Data presented as mean ± SEM. See *Results* for exact *P*-values.

II [control: 96.56 ± 7.135 µm^2; ethanol: 121.8 ± 10.82 µm^2; $t(35) = 2.030$, $P = 0.0500$, unpaired *t*-test]; Layer V/VI [Control: 147.4 ± 7.392 µm^2; ethanol: 142.4 ± 9.528 µm^2; $t(59) = 0.4211$, $P = 0.6752$, unpaired *t*-test]). These results, taken together, revealed a disruption of synaptic function and dendritic morphology that extended well beyond the immediate period ethanol exposure *in utero*.

The Effect of *In Utero* Exposure to Ethanol on Glu_{PSCs} Persisted Through P9-11

Pyramidal neurons release glutamate and receive glutamate-mediated synaptic currents from other pyramidal neurons (DeFelipe and Fariñas 1992). As observed at P6-8, the frequency of Glu_{PSCs} at P9-11 was significantly greater in layer V/VI pyramidal neurons in the ethanol-exposed compared to control somatosensory cortex (Fig. 6*B*,*D*; Control: 0.0078 ± 0.0024 Hz; ethanol: 0.0346 ± 0.0080 Hz; $P < 0.0001$, Mann–Whitney *U* test). However, the increase in the frequency of $GABA_{PSCs}$ at P6-8 was no longer evident (Fig. 6*A*,*C*; control: 0.09542 ± 0.0165 Hz; ethanol: 0.1276 ± 0.0274 Hz; $P = 0.6935$, Mann–Whitney *U* test). Thus, in the course of shaping cortical circuits, ethanol exposure *in utero* exerts a longer-lasting effect on glutamate-mediated vis-à-vis GABA-mediated synaptic transmission. Importantly, this persistent change in Glu_{PSC} frequency in layer V/VI pyramidal neurons resulted in a significant net increase in the ratio of $Glu_{PSCs}/GABA_{PSCs}$ frequency in the ethanol-exposed mice (Fig. 6*E*; control: 0.2396 ± 0.0727; ethanol: 0.6205 ± 0.1297; $P = 0.0211$, Mann–Whitney *U* test).

In layer II/III pyramidal neurons, and consistent with our observation at P6-8, *in utero* ethanol exposure did not affect the frequency of spontaneous $GABA_{PSCs}$ (Fig. 6*A*,*C*; Control: 0.0859 ± 0.0192 Hz; Ethanol: 0.0829 ± 0.0137 Hz; $P = 0.1111$, Mann–Whitney *U* test) or Glu_{PSCs} (Fig. 6*B*,*D*; control: 0.0247 ± 0.0061 Hz; ethanol: 0.0308 ± 0.0063 Hz; $P = 0.1792$, Mann–Whitney *U* test). In addition, the amplitude of $GABA_{PSCs}$ (Fig. 6*F*) and Glu_{PSCs} (Fig. 6*G*) monitored in either superficial or deep pyramidal neurons remained unaltered with *in utero* ethanol exposure (see Supplementary Table 6 for full statistics). As expected, $Glu_{PSCs}/GABA_{PSCs}$ ratio was unaffected in layer II/III pyramidal neurons (Fig. 6*E*; control: 0.9246 ± 0.2123; ethanol: 0.5990 ± 0.0802; $P = 0.7726$, Mann–Whitney *U* test). There were also no sex-associated differences between the control and ethanol-exposed cohort (Supplementary Fig. 2I–P; see Supplementary Table 7 for full statistics).

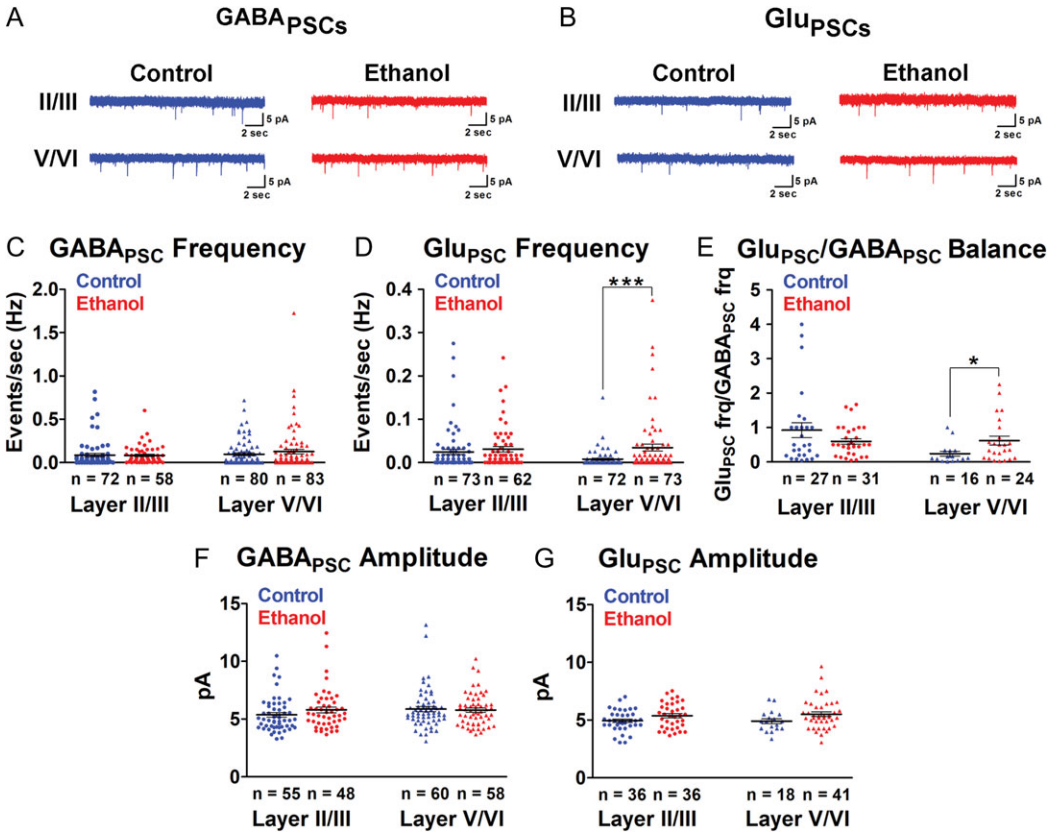

Figure 6. Binge-type ethanol exposure *in utero* increases spontaneous excitatory postsynaptic activity in the P9-11 somatosensory cortex. *A*, *B*: $GABA_{PSCs}$ (*A*) and Glu_{PSCs} (*B*) were monitored in layer II/III and layer V/VI pyramidal neurons in control (blue traces) and ethanol-exposed (red traces) somatosensory cortical slices. *C*, *D*: Mean frequency (Hz) of $GABA_{PSCs}$ (*C*) and Glu_{PSCs} (*D*) of layer II/III and layer V/VI pyramidal neurons in control (blue) and age-matched ethanol-exposed (red) cohorts. *E*: There was a significant difference in the $Glu_{PSCs}/GABA_{PSCs}$ ratio in the ethanol-exposed somatosensory cortex. *F*, *G*: There were no significant differences in the amplitude of $GABA_{PSCs}$ (*F*) or Glu_{PSCs} (*G*) between control (blue) and ethanol-exposed (red) cohorts. *n* = number of cells. Each dot represents data derived from one pyramidal cell. ***$P < 0.001$, *$P < 0.05$ (Mann–Whitney *U* test). Data presented as mean ± SEM. See *Results* for exact *P*-values for *C*–*E*. See Supplementary Table 6 for exact *P*-values for *F*, *G*.

The Effect of *In Utero* Exposure to Ethanol on Pyramidal Cell Morphology was Transient

In contrast to the functional changes, the disruptions in morphology were transient. In P9-11 somatosensory cortex, there were no longer differences in the complexity of apical dendrites in layer V/VI pyramidal neurons following exposure to ethanol *in utero* (Fig. 7A; ($F(1, 1159) = 0.2741$, $P = 0.6025$), repeated measures 2-way ANOVA, main effect of treatment), basal dendritic complexity (Fig. 7B; ($F(1, 960) = 0.1000$, $P = 0.7529$), repeated measures 2-way ANOVA, main effect of treatment), or apical dendritic length (Fig. 7C; control: 3067 ± 156.1 µm; ethanol: 3136 ± 181.7 µm; $t(61) = 0.2862$, $P = 0.7757$, unpaired *t*-test). Similarly, as was seen in the P6-8 cohort, there were no significant differences in layer II/III pyramidal neuron apical dendritic complexity (Fig. 7D; ($F(1, 405) = 0.0254$, $P = 0.8742$), repeated measures 2-way ANOVA, main effect of treatment), basal dendritic complexity (Fig. 7E: ($F(1, 540) = 0.8797$, $P = 0.3533$) repeated measures 2-way ANOVA, main effect of treatment), or apical dendritic length (Fig. 7C; control: 949.6 ± 54.76 µm; ethanol: 943.5 ± 54.30 µm; $t(45) = 0.0767$, $P = 0.9392$, unpaired *t*-test). Soma size was also not affected by exposure to ethanol *in utero* (Fig. 7F; Layer II/II [control: 101.5 ± 6.357 μm^2; ethanol: 103.5 ± 6.547 μm^2; $t(45) = 0.2246$, $P = 0.8233$, unpaired *t*-test]; Layer V/VI [control: 183.0 ± 9.320 μm^2; ethanol: 199.7 ± 11.09 μm^2; $t(61) = 1.154$, $P = 0.2529$, unpaired *t*-test]). In addition to dendritic morphology, the effect of *in utero* ethanol on migration was also transient. At postnatal Day 7, we found no significant differences in the density of YFP^+ layer V pyramidal neurons or $Cux1^+$ layer II/III pyramidal neurons in the somatosensory cortices of control and ethanol-exposed Thy1-YFP and wild-type mice, respectively (Supplementary Fig. 3B,D; $Cux1^+$ cell density in layer II/III [control: $0.00482 \pm 3.3\times10^{-4}$ cells/μm^2; ethanol: $0.00522 \pm 3.4\times10^{-4}$ cells/μm^2; $t(5) = 0.8081$, $P = 0.4558$, unpaired *t*-test]; YFP^+ cell density in layer V/VI [control: $3.8\times10^{-4} \pm 5.66\times10^{-5}$ cells/μm^2; ethanol: $3.0\times10^{-4} \pm 1.56\times10^{-5}$ cells/μm^2; $t(6) = 1.469$, $P = 0.1921$, unpaired *t*-test]). The thickness of the cortical layers was also similar between the control and ethanol-exposed somatosensory cortex, and thus did not affect density measurements (Supplementary Fig. 3C,E; Layer II/III thickness [control: 370.0 ± 9.199 µm; ethanol: 372.0 ± 9.288 µm; $t(5) = 0.1503$, $P = 0.8864$, unpaired *t*-test]; Layer V/VI thickness [control: 543.0 ± 18.38 µm; ethanol: 592.6 ± 33.91 µm; $t(6) = 1.286$, $P = 0.2458$, unpaired *t*-test]).

In Utero Ethanol Exposure Results in Tactile Sensory Deficits in Young Adolescent Mice

We next asked whether the abnormal form and function of pyramidal neurons in the somatosensory cortex consequent to *in utero* ethanol exposure is associated with sensory-related behavioral changes later in life. Indeed, individuals with FASD

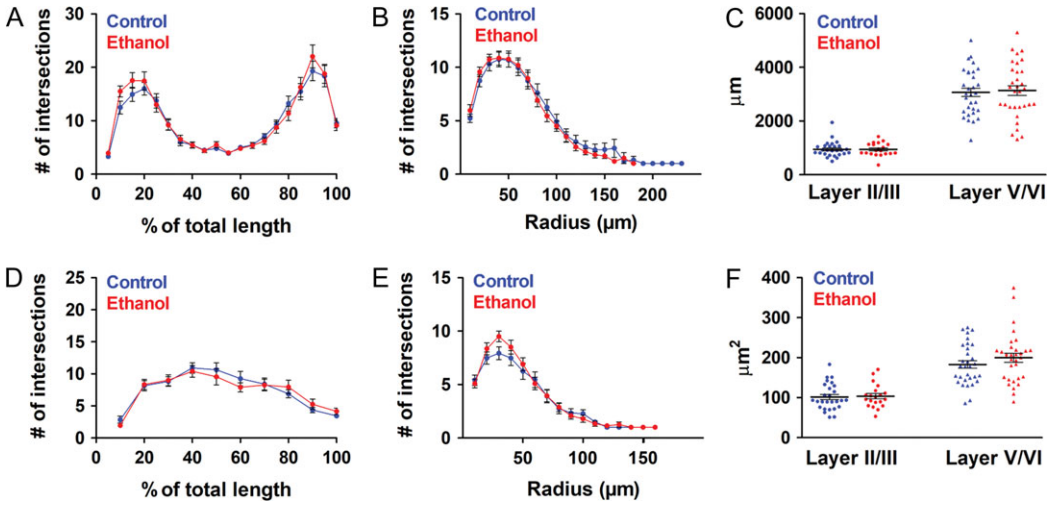

Figure 7. The altered pyramidal neuron dendritic complexity due to binge-type ethanol exposure *in utero* observed at P6-8 is not evident in the P9-11 somatosensory cortex. Sholl analysis of layer V/VI pyramidal neuron apical dendrite (*A*) and basal dendrites (*B*) and layer II/III pyramidal neuron apical dendrite (*D*) and basal dendrites (*E*) in control (blue lines) and ethanol-exposed (red lines) somatosensory cortex. Mean apical dendritic length (*C*) and soma size (*F*) in control (blue) and ethanol-exposed (red) layer II/III and layer V/VI pyramidal neurons. Layer II/III: (Control: $n = 27$; Ethanol: $n = 20$); Layer V/VI: (Control: $n = 31$; Ethanol: $n = 32$); n = number of cells. Each dot in (*C*) and (*F*) represents data derived from one pyramidal cell. *A*, *B*, *D*, *E*: Repeated measures 2-way ANOVA with Bonferroni post hoc test revealed no significant differences in dendritic complexity; *C*, *F*: unpaired *t*-test revealed no significant differences in apical dendritic length (*C*) or soma size (*F*). Data presented as mean ± SEM. See *Results* for exact *P*-values.

present with a host of sensory deficits (Franklin et al. 2008), mediated by the somatosensory cortex, including altered tactile sensitivity (Jirikowic et al. 2008, O'Malley and Rich 2013). In this light, we investigated tactile sensitivity in young adolescent mice (P21–P25) using the adhesive tape removal assay as described by Bouet et al. (2009); see *Methods*. As summarized graphically in Figure 8*C*, there was a significant increase in initial contact time, or the length of time for the ethanol-exposed mice to recognize the presence of the pieces of tape on their paws ($(F(1, 44) = 5.506$, $P = 0.0387)$, repeated measures 2-way ANOVA, main effect of treatment). There was no significant effect of sex on contact time in either the control (Fig. 8*E*; ($F(1, 40) = 0.1892$, $P = 0.6728$), repeated measures 2-way ANOVA, main effect of sex) or ethanol-exposed cohort (Fig. 8*F*; ($F(1, 48) = 0.4806$, $P = 0.5347$), repeated measures 2-way ANOVA, main effect of sex).

Following initial contact, mice continued grooming in attempts to remove the tape. For each animal, the latency to tape removal was recorded for both paws and used to calculate an average tape removal time per litter. The removal time, which has both a sensory and motor component, was overall similar between the control and ethanol-exposed cohorts (Fig. 8*D*; ($F(1, 44) = 0.9526$, $P = 0.3500$), repeated measures 2-way ANOVA, main effect of treatment). Thus, *in utero* binge-type ethanol exposure resulted in a subtle, yet significant, sensory dysfunction without disruption of sensorimotor ability.

Discussion

The premise driving this study is that the etiology underlying the cognitive and neurobehavioral impairments that define FASD are rooted early on as disturbances in the development of the embryonic brain. Using a mouse model of FASD based on a binge-type regimen of maternal ethanol consumption (Skorput et al. 2015), we investigated the effects of *in utero* exposure to ethanol on the disposition of radially migrating pyramidal neurons in the embryonic and postnatal mouse somatosensory cortex. We report that a relatively brief exposure of pregnant mice to ethanol that attains a blood alcohol level considered to be legally impaired in the USA (0.08%) can have short-term and lasting consequences on the development of pyramidal neurons in the somatosensory cortex of the fetal brain. The major findings are: (1) in the short-term, binge-type exposure to ethanol *in utero* delays the radial migration of primordial pyramidal neurons into the cortical plate of the embryonic somatosensory cortex; in the long-term, this is associated with (2) a transient effect on morphology and a persistent alteration in the synaptic function of pyramidal neurons, and (3) impaired tactile sensory processing, reminiscent of that observed in FASD individuals.

In Utero Exposure to Binge-Type Ethanol Disrupts the Distribution of Pyramidal Neurons During Radial Migration

Our *in utero* binge-type ethanol exposure paradigm targets a critical time in radial migration and selectively affects postmitotic pyramidal neurons in the embryonic somatosensory cortex. Specifically, *in utero* ethanol exposure resulted in a more dispersed pattern of $Tbr1^+$ immunofluorescence in the subplate. The subplate is formed as the first wave of radially migrating cortical plate-bound neurons splits the preplate into a superficial marginal zone and deeper subplate (Uylings et al. 1990; Allendoerfer and Shatz 1994; Parnavelas 2000; Nadarajah and Parnavelas 2002; Kriegstein and Noctor 2004; Marín-Padilla 2011). However, since preplate neurons also express Tbr1 (Bulfone et al. 1995; Hevner et al. 2001; Leone et al. 2008), the $Tbr1^+$ cells in the subplate likely included preplate-derived neurons. Nonetheless, given that both Tbr1 and Cux1 expression are altered, and the latter is expressed in precursor and migrating cells but not in native subplate neurons (Nieto et al. 2004; Molyneaux et al. 2007; Leone et al. 2008), we favor the interpretation that ethanol exposure *in utero* affected the migration of early- and late-born pyramidal neurons. Ethanol could have altered (1) the morphology of the RGCs, (2) the extent of their extension from the ventricular zone to the pial surface, (3) the

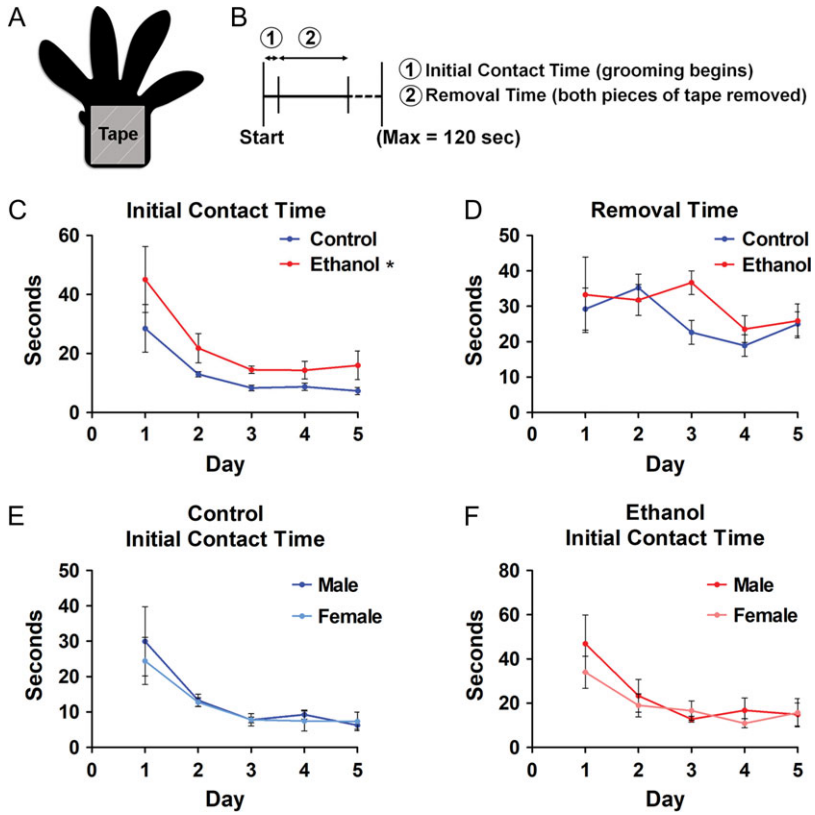

Figure 8. *In utero* ethanol exposure results in tactile sensory deficits in young adolescent mice. *A*: A ~4 × 6 mm piece of adhesive tape (gray square) is placed over the palm of the right and left forepaws of P21–25 mice. *B*: Experimental timeline delineating the latency of (1) tape recognition (initial contact time) and (2) removal of both pieces of tape (removal time). *C*, *D*: The contact time (*C*) and removal time (*D*) were measured for both control (blue lines) and ethanol-exposed (red lines) mice and there was a significant effect of treatment on contact time. *E*, *F*: There were no significant differences between males and females for control (*E*) or ethanol-exposed (*F*) mice. Control $n = 6$; ethanol $n = 7$; n = litters. All litters consisted of both male and female mice. $^*P < 0.05$ (repeated measures 2-way ANOVA with Bonferroni post hoc test). Data presented as mean ± SEM. See *Results* for exact *P*-values.

interaction between migrating neurons and the radial glial scaffolding, and/or (4) the detachment of neurons from the RGCs in the cortical plate (Rakic 1971, 1972; Anton et al. 1999; reviewed in Marín and Rubenstein 2003). Further studies will need to determine whether these and other processes (Ishii et al. 2017) contribute to an ethanol-induced defect in radial glia-guided migration.

In utero ethanol exposure did not affect IPCs since the control and ethanol-exposed cohorts showed a similar pattern of Tbr2 expression in the lower subventricular zone, and since the results of the BrdU and Ki67 assays did not indicate altered proliferation. However, we noted a decrease in Tbr2 immunofluorescence intensity in the upper subventricular zone. This may be accounted for by a delay in radial migration, or by IPCs expressing less Tbr2 in the ethanol-exposed somatosensory cortex. In addition, as differentiated IPC-derived neurons migrate away from the subventricular zone and downregulate Tbr2 (Englund et al. 2005), Tbr1 expression could be upregulated precociously, and this may underlie the observed increase in Tbr1 immunofluorescence intensity in the subplate of ethanol-exposed embryonic somatosensory cortex. It is unknown if *in utero* ethanol exposure affects the timing and transition of expression from one transcriptional marker to the next. Future work investigating this possibility would offer critical insight into the observed *in utero* ethanol-induced defects in radial migration.

The Effects of *In Utero* Ethanol Exposure are Directly Related to the Timing of Exposure During Gestation

The time and length of gestational exposure is a key determinant of the effects of *in utero* ethanol exposure (Maier et al. 1997, 1999). The timeline of our binge-type ethanol exposure (E13.5–E16.5) corresponds approximately to the mid-late first trimester and the beginning of the second trimester in humans (Clancy et al. 2001; Parnell et al. 2014). Importantly, both in humans (Sidman and Rakic 1973; Bystron et al. 2008) and in mice (Clancy et al. 2001), this time window overlaps with the period of radial migration. Commensurately, *in utero* ethanol exposure affected the radial migration of both early-born ($Tbr1^+$) and later-born ($Cux1^+$) primordial pyramidal neurons.

Our morphological and functional analysis point to binge-type ethanol exposure from E13.5–E16.5 targeting layer V/VI pyramidal neurons in the somatosensory cortex. The migration of the early-born, deep layer, pyramidal neurons peaks during the beginning of our ethanol exposure window, whereas the migration of later-born, upper layer, pyramidal neurons extends beyond the timeframe of exposure (Clancy et al. 2001). Our results are consistent with the notion that disruption of radial migration is dependent on the timing of binge-ethanol exposure *in utero*. Taking this view, we predict that a 3-day binge-ethanol exposure *in utero* at an earlier or later timeframe would affect subpopulations of early- or later-born pyramidal neurons.

Binge-Type *In Utero* Exposure to Ethanol Results in a Shift in the $Glu_{PSC}/GABA_{PSC}$ Ratio Despite a Recovery of Pyramidal Neuron Morphology

Hammer and Scheibel (1981) reported that deep layer pyramidal neurons of the somatosensory and motor cortices displayed decreased dendritic complexity in P0 rats exposed chronically to ethanol throughout gestation. It was speculated then that the abnormal morphology would not persist since ethanol may be delaying but not preventing dendritic growth (Hammer and Scheibel 1981). Here we present direct evidence to verify this speculation. Specifically, *in utero* exposure to binge-type ethanol transiently altered dendritic complexity in deep layer pyramidal neurons in the P6-8 somatosensory cortex. In rats, gestational exposure to ethanol also resulted in a transient alteration in dendritic complexity of pyramidal neurons (Lopez-Tejero et al. 1986). Overall, the normalization of pyramidal neuron morphology could reflect the speculated delay in development (Hammer and Scheibel 1981), or be due to plastic processes, such as dendritic sprouting and pruning, overriding or offsetting the effects of *in utero* ethanol exposure (Lindsley 2006).

The demonstration that ethanol exposure *in utero* results in lasting alterations in synaptic function despite normalization of pyramidal neuron morphology invokes the concept that form does not necessarily dictate or predict function, and vice versa. Abnormal morphology, even transiently manifested during the early stages of synaptogenesis, can imprint indelibly on the formation and shaping of neural circuits, leading to long-term functional consequences. This is further underscored by the persistent aberrance in function observed in this study despite recovery from migration defects (Supplementary Fig. 3). The increase in frequency but not in amplitude of spontaneous Glu_{PSCs} and $GABA_{PSCs}$ in deep layer pyramidal neurons points to a presynaptic effect. This could be due to changes in the number of synapses or increases in intraterminal calcium, leading to increased probability of vesicular fusion and neurotransmitter release. The findings of the present study call for future investigations on potential ethanol-induced changes in the number and maturity of spines, synaptic efficacy, and synaptic strength, as all of these could affect neurotransmission. Moreover, a shift in the $Glu_{PSCs}/GABA_{PSCs}$ balance favoring Glu_{PSCs} in the ethanol-exposed P9-11 somatosensory cortex foreshadows a potential E/I imbalance that favors excitation later in development. FASD has been postulated to be a disorder of E/I imbalance within neural circuits (Skorput et al. 2015; reviewed in Sadrian et al. 2013), that could underlie the increased incidence of seizures reported in affected FASD individuals (Bell et al. 2010).

In Utero Ethanol Exposure is Associated with Deficits in Sensory Processing

Dysfunctional sensory processing is a hallmark of FASD (Franklin et al. 2008; Jirikowic et al. 2008; Carr et al. 2010). The tape removal test applied to mice assesses the mouth and forepaws for sensory and motor abilities (Bouet et al. 2009). In our study, this test revealed diminished tactile sensitivity but not motoric ability in young adolescent mice exposed to binge-type *in utero* ethanol. While this is clinically consistent with an overall "underresponsivity" to stimuli (Franklin et al. 2008; Jirikowic et al. 2008; Carr et al. 2010), it is also common for children with FASD to present with tactile defensiveness, or hypersensitivity to touch (Jirikowic et al. 2008). The results presented here demonstrate disrupted tactile sensitivity in a mouse model for FASD, and specifically highlight the enduring and detrimental effects of a short-term and binge-type exposure to ethanol *in utero*.

Conclusion

The myriad behavioral and cognitive deficits associated with FASD (Streissguth et al. 1991; Mattson and Riley 1998; Mattson et al. 1998; Riley and McGee 2005; Franklin et al. 2008; Jirikowic et al. 2008; Carr et al. 2010) implies that prenatal ethanol exposure targets the developing brain, including the somatosensory cortex. Indeed, the data presented here strongly implicate the somatosensory cortex as a brain region targeted by ethanol exposure *in utero*. Our study provides the groundwork for interrogating whether or not our findings in the somatosensory cortex apply to other brain regions that have been implicated in contributing to the underpinnings of FASD, such as the prefrontal and motor cortices (Miller 1986; Miller and Dow-Edwards 1988; Abernathy et al. 2010; Xie et al. 2010; Skorput et al. 2015, Skorput and Yeh 2016). Taken together, these findings contribute to our understanding of the embryonic etiology of FASD and inform further investigations of the effects of prenatal ethanol exposure on cortical development.

Supplementary Material

Supplementary material is available at *Cerebral Cortex* online.

Funding

This work was supported by the National Institute on Alcohol Abuse and Alcoholism at the National Institutes of Health (PHS NIH R01 AA-023410 to H.H.Y., PHS NIH R21 AA-024036 to H.H.Y., PHS NIH F30 AA025534 to L.C.D). The authors thank the Microscopy—Irradiation, Pre-clinical Imaging and Microscopy Resource at the Norris Cotton Cancer Center at Dartmouth with NCI Cancer Center Support Grant (PHS NIH 5P30 CA023108-37) for the use of the confocal microscopy facility.

Notes

Marielle Brady and Kathleen Raty assisted with data collection for Supplementary Fig. 3. *Conflict of Interest*: None declared.

References

Abernathy K, Chandler LJ, Woodward JJ. 2010. Alcohol and the prefrontal cortex. Int Rev Neurobiol. 91:289–320.

Allendoerfer KL, Shatz CJ. 1994. The subplate, a transient neocortical structure: its role in the development of connections between thalamus and cortex. Annu Rev Neurosci. 17:185–218.

Amaral DG. 2013. The functional organization of perception and movement. In: Kandel ER, Schwartz JH, Jessell TM, Siegelbaum SA, Hudspeth AJ, editors. Principles of neural science. 5th ed. New York (NY): McGraw-Hill. p. 356–369.

Andersen SL. 2003. Trajectories of brain development: point of vulnerability or window of opportunity? Neurosci Biobehav Rev. 27:3–18.

Angevine JB, Sidman RL. 1961. Autoradiographic study of cell migration during histogenesis of cerebral cortex in the mouse. Nature. 192:766–768.

Anton ES, Kreidberg JA, Rakic P. 1999. Distinct functions of α_3 and α_v integrin receptors in neuronal migration and laminar organization of the cerebral cortex. Neuron. 22:277–289.

Astley SJ. 2013. Validation of the fetal alcohol spectrum disorder (FASD) 4-digit diagnostic code. J Popul Ther Clin Pharmacol. 20:e416–e467.

Astley SJ, Clarren SK. 2000. Diagnosing the full spectrum of fetal alcohol-exposed individuals: introducing the 4-digit diagnostic code. Alcohol Alcohol. 35:400–410.

Bell SH, Stade B, Reynolds JN, Rasmussen C, Andrew G, Hwang PA, Carlen PL. 2010. The remarkably high prevalence of epilepsy and seizure history in fetal alcohol spectrum disorders. Alcohol Clin Exp Res. 34:1084–1089.

Ben-Ari Y. 2002. Excitatory actions of GABA during development: the nature of the nurture. Nat Rev Neurosci. 3:728–739.

Ben-Ari Y, Cherubini E, Corradetti R, Gaiarsa JL. 1989. Giant synaptic potentials in immature rat CA3 hippocampal neurones. J Physiol (Lond). 416:303–325.

Blue ME, Parnavelas JG. 1983. The formation and maturation of synapses in the visual cortex of the rat. I. Qualitative analysis. J Neurocytol. 12:599–616.

Bouet V, Boulouard M, Toutain J, Divoux D, Bernaudin M, Schumann-Bard P, Freret T. 2009. The adhesive removal test: a sensitive method to assess sensorimotor deficits in mice. Nat Protoc. 4:1560–1564.

Bulfone A, Smiga SM, Shimamura K, Peterson A, Puelles L, Rubenstein JLR. 1995. T-Brain-1: a homolog of Brachyury whose expression defines molecularly distinct domains within the cerebral cortex. Neuron. 15:63–78.

Bystron I, Blakemore C, Rakic P. 2008. Development of the human cerebral cortex: Boulder Committee revisited. Nat Rev Neurosci. 9:110–122.

Carr JL, Agnihotri S, Keightley M. 2010. Sensory processing and adaptive behavior deficits of children across the fetal alcohol spectrum disorder continuum. Alcohol Clin Exp Res. 34: 1022–1032.

Cherubini E, Gaiarsa JL, Ben-Ari Y. 1991. GABA: an excitatory transmitter in early postnatal life. Trends Neurosci. 14: 515–519.

Clancy B, Darlington RB, Finlay BL. 2001. Translating developmental time across mammalian species. Neuroscience. 105: 7–17.

Custo Greig LF, Woodworth MB, Galazo MJ, Padmanabhan H, Macklis JD. 2013. Molecular logic of neocortical projection neuron specification, development and diversity. Nat Rev Neurosci. 14:755–769.

Cuzon VC, Yeh PW, Yanagawa Y, Obata K, Yeh HH. 2008. Ethanol consumption during early pregnancy alters the disposition of tangentially migrating GABAergic interneurons in the fetal cortex. J Neurosci. 28:1854–1864.

DeFelipe J, Fariñas I. 1992. The pyramidal neuron of the cerebral cortex: morphological and chemical characteristics of the synaptic inputs. Prog Neurobiol. 39:563–607.

Englund C, Fink A, Lau C, Pham D, Daza RAM, Bulfone A, Kowalczyk T, Hevner RF. 2005. Pax6, Tbr2, and Tbr1 are expressed sequentially by radial glia, intermediate progenitor cells, and postmitotic neurons in developing neocortex. J Neurosci. 25:247–251.

Feng G, Mellor RH, Bernstein M, Keller-Peck C, Nguyen QT, Wallace M, Nerbonne JM, Lichtman JW, Sanes JR. 2000. Imaging neuronal subsets in transgenic mice expressing multiple spectral variants of GFP. Neuron. 28:41–51.

Franklin L, Deitz J, Jirikowic T, Astley S. 2008. Children with fetal alcohol spectrum disorders: problem behaviors and sensory processing. Am J Occup Ther. 62:265–273.

Gerdes J, Lemke H, Baisch H, Wacker HH, Schwab U, Stein H. 1984. Cell cycle analysis of a cell proliferation-associated human nuclear antigen defined by the monoclonal antibody Ki-67. J Immunol. 133:1710–1715.

Gratzner HG. 1982. Monoclonal antibody to 5-bromo- and 5-iododeoxyuridine: a new reagent for detection of DNA replication. Science. 218:474–475.

Götz M, Stoykova A, Gruss P. 1998. Pax6 controls radial glia differentiation in the cerebral cortex. Neuron. 21:1031–1044.

Hammer RP, Scheibel AB. 1981. Morphologic evidence for a delay of neuronal maturation in fetal alcohol exposure. Exp Neurol. 74:587–596.

Hevner RF, Shi L, Justice N, Hsueh YP, Sheng M, Smiga S, Bulfone A, Goffinet AM, Campagnoni AT, Rubenstein JL. 2001. Tbr1 regulates differentiation of the preplate and layer 6. Neuron. 29:353–366.

Ishii S, Torri M, Son AI, Rajendraprasad M, Morozov YM, Kawasawa YI, Salzberg AC, Fujimoto M, Brennand K, Nakai A, et al. 2017. Variations in brain defects result from cellular mosaicism in the activation of heat shock signaling. Nat Commun. 8:15157.

Jirikowic T, Olson HC, Kartin D. 2008. Sensory processing, school performance, and adaptive behavior of young school-age children with fetal alcohol spectrum disorders. Phys Occup Ther Pediatr. 28:117–136.

Johnson R, Armstrong-James M. 1970. Morphology of superficial postnatal cerebral cortex with special reference to synapses. Z Zellforsch Mikrosk Anat. 110:540–558.

Kee N, Sivalingam S, Boonstra R, Wojtowicz JM. 2002. The utility of Ki-67 and BrdU as proliferative markers of adult neurogenesis. J Neurosci Methods. 115:97–105.

Kriegstein A, Alvarez-Buylla A. 2009. The glial nature of embryonic and adult neural stem cells. Annu Rev Neurosci. 32:149–184.

Kriegstein AR, Noctor SC. 2004. Patterns of neuronal migration in the embryonic cortex. Trends Neurosci. 27:392–399.

Leone DP, Srinivasan K, Chen B, Alcamo E, McConnell SK. 2008. The determination of projection neuron identity in the developing cerebral cortex. Curr Opin Neurobiol. 18:28–35.

Lieber CS, DeCarli LM. 1989. Liquid diet technique of ethanol administration: 1989 update. Alcohol Alcohol. 24:197–211.

Lindsley TA. 2006. Effects of ethanol on mechanisms regulating neuronal process outgrowth. In: Miller MW, editor. Brain development: normal processes and the effects of alcohol and nicotine. New York (NY): Oxford University Press. p. 230–244.

Lopez-Tejero D, Ferrer I, Llobera M, Herrera E. 1986. Effects of prenatal ethanol exposure on physical growth, sensory reflex maturation and brain development in the rat. Neuropathol Appl Neurobiol. 12:251–260.

Maier SE, Chen WJA, Miller JA, West JR. 1997. Fetal alcohol exposure and temporal vulnerability: regional differences in alcohol-induced microencephaly as a function of the timing of binge-like alcohol exposure during rat brain development. Alcohol Clin Exp Res. 21:1418–1428.

Maier SE, Miller JA, Blackwell JM, West JR. 1999. Fetal alcohol exposure and temporal vulnerability: regional differences in cell loss as a function of the timing of binge-like alcohol exposure during brain development. Alcohol Clin Exp Res. 23:726–734.

Maier SE, West JR. 2001. Drinking patterns and alcohol-related birth defects. Alcohol Res Health. 25:168–174.

Marín O, Rubenstein JLR. 2003. Cell migration in the forebrain. Annu Rev Neurosci. 26:441–483.

Marín-Padilla M. 1978. Dual origin of the mammalian neocortex and evolution of the cortical plate. Anat Embryol. 152: 109–126.

Marín-Padilla M. 2011. Mammalian cerebral cortex: embryonic development and cytoarchitecture. In: Marín-Padilla M, editor. The human brain: prenatal development and structure. Heidelberg (Germany): Springer. p. 5–10.

Mattson SN, Riley EP. 1998. A review of the neurobehavioral deficits in children with fetal alcohol syndrome or prenatal exposure to alcohol. Alcohol Clin Exp Res. 22:279–294.

Mattson SN, Riley EP, Gramling L, Delis DC, Jones KL. 1998. Neuropsychological comparison of alcohol-exposed children with or without physical features of fetal alcohol syndrome. Neuropsychology. 12:146–153.

McClain JA, Hayes DM, Morris SA, Nixon K. 2011. Adolescent binge alcohol exposure alters hippocampal progenitor cell proliferation in rats: effects on cell cycle kinetics. J Comp Neurol. 519:2697–2710.

Meller K, Breipohl W, Glees P. 1968. Synaptic organization of the molecular and the outer granular layer in the motor cortex in the white mouse during postnatal development. A Golgi- and electronmicroscopical study. Z Zellforsch Mikrosk Anat. 92: 217–231.

Miller MW. 1986. Effects of alcohol on the generation and migration of cerebral cortical neurons. Science. 233:1308–1311.

Miller MW. 1988. Effect of prenatal exposure to ethanol on the development of cerebral cortex: I. Neuronal generation. Alcohol Clin Exp Res. 12:440–449.

Miller MW, Chiaia NL, Rhoades RW. 1990. Intracellular recording and injection study of corticospinal neurons in the rat somatosensory cortex: effect of prenatal exposure to ethanol. J Comp Neurol. 297:91–105.

Miller MW, Dow-Edwards DL. 1988. Structural and metabolic alterations in rat cerebral cortex induced by prenatal exposure to ethanol. Brain Res. 474:316–326.

Mione MC, Cavanagh JFR, Harris B, Parnavelas JG. 1997. Cell fate specification and symmetrical/asymmetrical divisions in the developing cerebral cortex. J Neurosci. 17:2018–2029.

Molyneaux BJ, Arlotta P, Menezes JRL, Macklis JD. 2007. Neuronal subtype specification in the cerebral cortex. Nat Rev Neurosci. 8:427–437.

Nadarajah B, Parnavelas JG. 2002. Modes of neuronal migration in the developing cerebral cortex. Nat Rev Neurosci. 3: 423–432.

Nieto M, Monuki ES, Tang H, Imitola J, Haubst N, Khoury SJ, Cunningham J, Gotz M, Walsh CA. 2004. Expression of Cux-1 and Cux-2 in the subventricular zone and upper layers II–IV of the cerebral cortex. J Comp Neurol. 479:168–180.

Nixon K, Crews FT. 2004. Temporally specific burst in cell proliferation increases hippocampal neurogenesis in protracted abstinence from alcohol. J Neurosci. 24:9714–9722.

Noctor SC, Martínez-Cerdeño V, Ivic L, Kriegstein AR. 2004. Cortical neurons arise in symmetric and asymmetric division zones and migrate through specific phases. Nat Neurosci. 7:136–144.

Obata K, Oide M, Tanaka H. 1978. Excitatory and inhibitory actions of GABA and glycine on embryonic chick spinal neurons in culture. Brain Res. 144:179–184.

Oh S, Lee D, Kim T, Kim TS, Oh HJ, Hwang CY, Kong YY, Kwon KS, Lim DS. 2009. Crucial role for Mst1 and Mst2 kinases in early embryonic development of the mouse. Mol Cell Biol. 29:6309–6320.

Owens DF, Kriegstein AR. 2002. Is there more to GABA than synaptic inhibition? Nat Rev Neurosci. 3:715–727.

O'Malley KD, Rich SD. 2013. Clinical implications of a link between fetal alcohol spectrum disorders (FASD) and Autism or Asperger's Disorder—a neurodevelopmental frame for helping understanding and management Ch. 20. In: Fitzgerald M, editor. Recent advances in Autism spectrum disorders. Vol I. InTech. p. 451–477.

Parnavelas JG. 2000. The origin and migration of cortical neurones: new vistas. Trends Neurosci. 23:126–131.

Parnell SE, Holloway HE, Baker LK, Styner MA, Sulik KK. 2014. Dysmorphogenic effects of first trimester equivalent ethanol exposure in mice: a magnetic resonance microscopy-based study. Alcohol Clin Exp Res. 38:2008–2014.

Preibisch S, Saalfeld S, Tomancak P. 2009. Globally optimal stitching of tiled 3D microscopic image acquisitions. Bioinformatics. 25:1463–1465.

Rakic P. 1971. Guidance of neurons migrating to the fetal monkey neocortex. Brain Res. 33:471–476.

Rakic P. 1972. Mode of cell migration to the superficial layers of fetal monkey neocortex. J Comp Neurol. 145:61–83.

Rakic P. 1974. Neurons in rhesus monkey visual cortex: systematic relation between time of origin and eventual disposition. Science. 183:425–427.

Riley EP, McGee CL. 2005. Fetal alcohol spectrum disorders: an overview with emphasis on changes in brain and behavior. Exp Biol Med. 230:357–365.

Sadrian B, Wilson DA, Saito M. 2013. Long-lasting neural circuit dysfunction following developmental ethanol exposure. Brain Sci. 3:704–727.

Schindelin J, Arganda-Carreras I, Frise E, Kaynig V, Longair M, Pietzsch T, Preibisch S, Rueden C, Saalfeld S, Schmid B, et al. 2012. Fiji: an open-source platform for biological-image analysis. Nat Methods. 9:676–682.

Schneider CA, Rasband WS, Eliceiri KW. 2012. NIH Image to ImageJ: 25 years of image analysis. Nat Methods. 9:671–675.

Scholzen T, Gerdes J. 2000. The Ki-67 protein: from the known and the unknown. J Cell Physiol. 182:311–322.

Sholl DA. 1953. Dendritic organization in the neurons of the visual and motor cortices of the cat. J Anat. 87:387–406.

Sidman RL, Rakic P. 1973. Neuronal migration, with special reference to developing human brain: a review. Brain Res. 62:1–35.

Skorput AG, Gupta VP, Yeh PW, Yeh HH. 2015. Persistent interneuronopathy in the prefrontal cortex of young adult offspring exposed to ethanol *in utero*. J Neurosci. 35:10977–10988.

Skorput AG, Yeh HH. 2016. Chronic gestational exposure to ethanol leads to enduring aberrances in cortical form and function in the medial prefrontal cortex. Alcohol Clin Exp Res. 40:1479–1488.

Stratman JL, Barnes WM, Simon TC. 2003. Universal PCR genotyping assay that achieves single copy sensitivity with any primer pair. Transgenic Res. 12:521–522.

Streissguth AP, Aase JM, Clarren SK, Randels SP, LaDue RA, Smith DF. 1991. Fetal alcohol syndrome in adolescents and adults. JAMA. 265:1961–1967.

Tan CH, Denny CH, Cheal NE, Sniezek JE, Kanny D. 2015. Alcohol use and binge drinking among women of childbearing age—United States, 2011–2013. MMWR Morb Mortal Wkly Rep. 64:1042–1046.

Uylings HB, Van Eden CG, Parnavelas JG, Kalsbeek A. 1990. The prenatal and postnatal development of rat cerebral cortex. In: Kolb B, Tees RC, editors. The cerebral cortex of the rat. Cambridge (Massachusetts): MIT Press. p. 35–76.

Xie N, Qiuhong Y, Chappell TD, Li CX, Waters RS. 2010. Prenatal alcohol exposure reduces the size of the forelimb representation in motor cortex in rat: an intracortical microstimulation (ICMS) mapping study. Alcohol. 44:185–194.